

Experimental verification of the partial mixing model

Raghavan Parthasarathy

I hereby release this thesis to the public. I understand that this thesis will be made available from the OhioLINK ETD Center and the Adair Library Circulation Desk for public access. I also authorize individuals to make copies of this thesis as needed for scholarly research.

by

Raghavan Parthasarathy

Submitted in Partial Fulfillment of the Requirements

Signature: 

for the Degree of

Master of Science

in the

Approvals: 

Geological and Environmental Science

Program

Dr. Isam Ateia, Thesis Advisor



Dr. Douglas M. Price, Thesis Co-Advisor



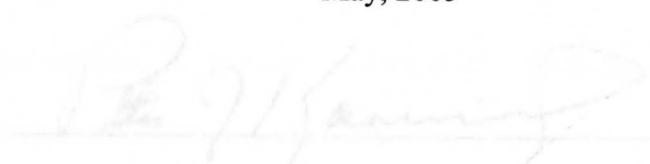
Dr. Alan M. Jacobs, Committee Member



YOUNGSTOWN STATE UNIVERSITY

Mr. Scott C. Williams, Committee Member

May, 2005

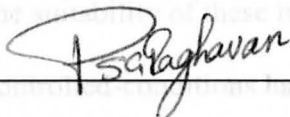


Peter J. Kawlousky, Dean of Graduate Studies and Research

Experimental Verification of the partial mixing model

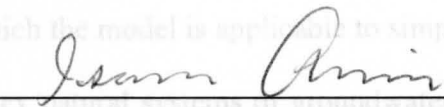
Raghavan Parthasarathy

I hereby release this thesis to the public. I understand that this thesis will be made available from the OhioLINK ETD Center and the Maag Library Circulation Desk for public access. I also authorize the University or other individuals to make copies of this thesis as needed for scholarly research.

Signature:  5/3/05

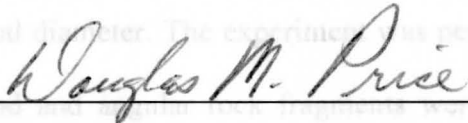
Raghavan Parthasarathy, Student

Date

Approvals:  5/3/05

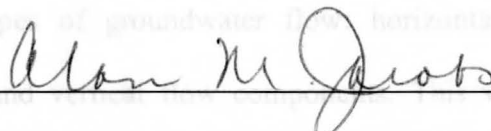
Dr. Isam Amin, Thesis Advisor

Date

 5/3/05

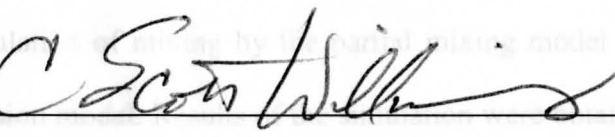
Dr. Douglas M. Price, Thesis Co-Advisor

Date

 5/3/05

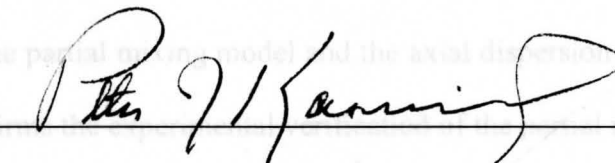
Dr. Alan M. Jacobs, Committee Member

Date

 5/4/05

Mr. Scott C. Williams, Committee Member

Date

 5/6/05

Peter J. Kasvinsky, Dean of Graduate Studies and Research

Date

ABSTRACT

Several tracer mathematical models such as the piston flow model, perfect mixing model, partial mixing model, dispersive models and discrete-state compartment models are currently used to calculate residence times of groundwater, typically between recharge and discharge areas. These models are based on theoretical considerations that are not subjected to experimental verification prior to their application in field studies. Therefore, the suitability of these tracer models to complex field situations or even simple laboratory controlled-conditions has not been experimentally documented.

This study experimentally verifies the partial mixing model. It determines the extent to which the model is applicable to simple laboratory conditions and ultimately the more complex natural systems of groundwater. The objective is achieved by simulating groundwater flow through porous media using a packed column, one meter in length and 15cm internal diameter. The experiment was performed using two flow rates, 25 and 50 ml/min. Sand and angular rock fragments were used separately as packing materials. Sodium chloride was used as a tracer. Verification of the model was conducted for three different types of groundwater flow: horizontal flow, vertical flow and flow with horizontal and vertical flow components. This was achieved by orienting the packed column in the horizontal, vertical and inclined positions, respectively.

Simulation of mixing by the partial mixing model was compared to that of the axial dispersion model. Results of the simulation were obtained by fitting the two models to the experimental data obtained from the packed column. Results of the two models show that the partial mixing model and the axial dispersion model behave similarly. This further confirms the experimental verification of the partial mixing model.

DEDICATION

	PAGE
This thesis is dedicated with love and affection to	
my parents	
Dr. R. Parthasarathy and Mrs. Malathi Parthasarathy	
ACKNOWLEDGEMENTS	xvii
LIST OF TABLES	viii
LIST OF FIGURES	xi
CHAPTER 1	
1.0 INTRODUCTION	1
1.1 Groundwater residence time	1
1.2 Current tracer mathematical models	2
1.3 Statement of the problem	3
1.4 Objective	3
CHAPTER 2	
2.0 LITERATURE REVIEW AND THEORETICAL BACKGROUND	5
2.1 Lumped parameter models	5
2.2 Models and their hydrogeological significance	8
2.3 Determination of the mean transit time by the lumped parameter approach	8
2.4 Partial mixing	10

TABLE OF CONTENTS

	PAGE
ACKNOWLEDGEMENTS	xvii
LIST OF TABLES	viii
LIST OF FIGURES	xi
CHAPTER 1	
1.0 INTRODUCTION	1
1.1 Groundwater residence time	1
1.2 Current tracer mathematical models	2
4.2.1 Horizontal position with sand packing	
1.3 Statement of the problem	3
– Flow rate: 25 ml/min	21
1.4 Objective	3
4.2.2 Vertical position with sand packing	
– Flow rate: 25 ml/min	26
4.2.3 Inclined position with sand packing	
– Flow rate: 25 ml/min	32
4.2.4 Horizontal position with sand packing	
– Flow rate: 50 ml/min	38
4.2.5 Vertical position with sand packing	
– Flow rate: 50 ml/min	44
4.2.6 Inclined position with sand packing	
– Flow rate: 50 ml/min	50
CHAPTER 2	
2.0 LITERATURE REVIEW AND THEORETICAL BACKGROUND	5
2.1 Lumped parameter models	5
2.2 Models and their hydrogeological significance	8
2.3 Determination of the mean transit time by the lumped parameter approach	8
2.4 Partial mixing	10

CHAPTER 3	
3.0 METHODS AND PROCEDURES	12
3.1 Introduction	12
3.2 Experimental apparatus	15
3.3 Impulse tracer injection - The partial mixing model	16
– Flow rate: 25 ml/min	68
CHAPTER 4	
4.0 RESULTS AND DISCUSSIONS	19
4.1 Introduction	19
4.2 Experimental runs	20
4.2.1 Horizontal position with sand packing	
– Flow rate: 25 ml/min	21
4.2.2 Vertical position with sand packing	26
– Flow rate: 25 ml/min	
4.2.3 Inclined position with sand packing	
– Flow rate: 25 ml/min	32
4.2.4 Horizontal position with sand packing	38
– Flow rate: 50 ml/min	
4.2.5 Vertical position with sand packing	
– Flow rate: 50 ml/min	44
4.2.6 Inclined position with sand packing	
– Flow rate: 50 ml/min	50

	4.2.7 Horizontal position with angular rock fragments packing	
	– Flow rate: 25 ml/min	56
Table 4.1	4.2.8 Vertical position with angular rock fragments packing	60
	– Flow rate: 25 ml/min (probe 1)	
	– Flow rate: 25 ml/min	62
Table 4.2	Horizontal position with sand packing	62
	4.2.9 Inclined position with angular rock fragments packing	
Table 4.3	Horizontal – Flow rate: 25 ml/min packing	68
	– Flow rate: 25 ml/min (probe 1)	
	4.2.10 Horizontal position with angular rock fragments packing	
Table 4.4	Vertical position with sand packing	70
	– Flow rate: 50 ml/min	74
Table 4.5	4.2.11 Vertical position with angular rock fragments packing	78
	– Flow rate: 25 ml/min (probe 1)	
	– Flow rate: 50 ml/min	80
Table 4.6	Vertical position with sand packing	80
	4.2.12 Inclined position with angular rock fragments packing	
Table 4.7	Incline – Flow rate: 50 ml/min packing	86
	– Flow rate: 25 ml/min (probe 1)	
	4.3 Discussion	92
Table 4.8	Inclined position with sand packing	94
	– Flow rate: 25 ml/min (probe 2)	
CHAPTER 5	Inclined position with sand packing	96
	– Flow rate: 25 ml/min (probe 1)	
5.0 CONCLUSIONS AND RECOMMENDATIONS		100
Table 4.10	Horizontal position with sand packing	38
	– Flow rate: 50 ml/min (probe 1)	100
Table 4.11	5.1 Future recommendations with sand packing	101
	– Flow rate: 50 ml/min (probe 2)	
Table 4.12	Horizontal position with sand packing	42
REFERENCES	– Flow rate: 50 ml/min (probe 3)	104
Table 4.13	Vertical position with sand packing	44
	– Flow rate: 50 ml/min (probe 1)	
Table 4.14	Vertical position with sand packing	46
	– Flow rate: 50 ml/min (probe 2)	

LIST OF TABLES

<u>TABLE</u>	<u>TITLE</u>	<u>PAGE</u>
Table 4.1:	Horizontal position with sand packing - Flow rate: 25 ml/min (probe 1)	20
Table 4.2	Horizontal position with sand packing - Flow rate: 25 ml/min (probe 2)	22
Table 4.3	Horizontal position with sand packing - Flow rate: 25 ml/min (probe 3)	24
Table 4.4	Vertical position with sand packing - Flow rate: 25 ml/min (probe 1)	26
Table 4.5	Vertical position with sand packing - Flow rate: 25 ml/min (probe 2)	28
Table 4.6	Vertical position with sand packing - Flow rate: 25 ml/min (probe 3)	30
Table 4.7	Inclined position with sand packing - Flow rate: 25 ml/min (probe 1)	32
Table 4.8	Inclined position with sand packing - Flow rate: 25 ml/min (probe 2)	34
Table 4.9	Inclined position with sand packing - Flow rate: 25 ml/min (probe 3)	36
Table 4.10	Horizontal position with sand packing - Flow rate: 50 ml/min (probe 1)	38
Table 4.11	Horizontal position with sand packing - Flow rate: 50 ml/min (probe 2)	40
Table 4.12	Horizontal position with sand packing - Flow rate: 50 ml/min (probe 3)	42
Table 4.13	Vertical position with sand packing - Flow rate: 50 ml/min (probe 1)	44
Table 4.14	Vertical position with sand packing - Flow rate: 50 ml/min (probe 2)	46

<u>TABLE</u>	<u>TITLE</u>	<u>PAGE</u>
Table 4.15	Vertical position with sand packing – Flow rate: 50 ml/min (probe 3)	48
Table 4.16	Inclined position with sand packing – Flow rate: 50 ml/min (probe 1)	50
Table 4.17	Inclined position with sand packing – Flow rate: 50 ml/min (probe 2)	52
Table 4.18	Inclined position with sand packing – Flow rate: 50 ml/min (probe 3).	54
Table 4.19	Horizontal position with angular rock fragments packing – Flow rate: 25ml/min (probe 1)	56
Table 4.20	Horizontal position with angular rock fragments packing – Flow rate: 25 ml/min (probe 2)	58
Table 4.21	Horizontal position with angular rock fragments packing – Flow rate: 25 ml/min (probe 3)	60
Table 4.22	Vertical position with angular rock fragments packing – Flow rate: 25 ml/min (probe 1)	62
Table 4.23	Vertical position with angular rock fragments packing – Flow rate: 25 ml/min (probe 2)	64
Table 4.24	Vertical position with angular rock fragments packing – Flow rate: 25 ml/min (probe 3)	66
Table 4.25	Inclined position with angular rock fragments packing – Flow rate: 25 ml/min (probe 1)	68
Table 4.26	Inclined position with angular rock fragments packing – Flow rate: 25 ml/min (probe 2)	70
Table 4.27	Inclined position with angular rock fragments packing – Flow rate: 25 ml/min (probe 3)	72
Table 4.28	Horizontal position with angular rock fragments packing – Flow rate: 50 ml/min (probe 1)	74
Table 4.29	Horizontal position with angular rock fragments packing – Flow rate: 50 ml/min (probe 2)	76

<u>TABLE</u>	<u>TITLE</u>	<u>PAGE</u>
Table 4.30	Horizontal position with angular rock fragments packing – Flow rate: 50 ml/min (probe 3)	78
Figure 3.1 a	Picture of column in horizontal position	13
Table 4.31	Vertical position with angular rock fragments packing – Flow rate: 50 ml/min (probe 1)	80
Figure 3.1 b	Picture of column in vertical position	13
Table 4.32	Vertical position with angular rock fragments packing – Flow rate: 50 ml/min (probe 2)	82
Figure 3.2 a	Picture of column in vertical position	13
Figure 3.2 b	Vertical position of packed column	13
Table 4.33	Vertical position with angular rock fragments packing – Flow rate: 50 ml/min (probe 3)	84
Figure 3.3 a	Picture of column in vertical position	14
Table 4.34	Inclined position with angular rock fragments packing – Flow rate: 50 ml/min (probe 1)	86
Figure 4.1	Fitting of the partial mixing model and axial dispersion model to the experimental curve for probe 1 of the column in inclined position with sand packing and a flow rate of 25 ml/min	21
Table 4.35	Inclined position with angular rock fragments packing – Flow rate: 50 ml/min (probe 2)	88
Figure 4.2	Fitting of the partial mixing model and axial dispersion model to the experimental curve for probe 2 of the column in inclined position with sand packing and a flow rate of 25 ml/min	21
Table 4.36	Inclined position with angular rock fragments packing – Flow rate: 50 ml/min (probe 3)	90
Figure 4.3	Fitting of the partial mixing model and axial dispersion model to the experimental curve for probe 3 of the column in inclined position with sand packing and a flow rate of 25 ml/min	21
Table 4.37	Experimental residence times in comparison with calculated residence time.	94
Figure 4.3	Fitting of the partial mixing model and axial dispersion model to the experimental curve for probe 3 of the column in horizontal position with sand packing and a flow rate of 25 ml/min	25
Figure 4.4	Fitting of the partial mixing model and axial dispersion model to the experimental curve for probe 1 of the column in vertical position with sand packing and a flow rate of 25 ml/min	27
Figure 4.5	Fitting of the partial mixing model and axial dispersion model to the experimental curve for probe 2 of the column in vertical position with sand packing and a flow rate of 25 ml/min	29
Figure 4.6	Fitting of the partial mixing model and axial dispersion model to the experimental curve for probe 3 of the column in vertical position with sand packing and a flow rate of 25 ml/min	31

LIST OF FIGURES

<u>FIGURE</u>	<u>TITLE</u>	<u>PAGE</u>
Figure 3.1 a	Picture of column in horizontal position	12
Figure 3.1 b	Horizontal position of packed column	13
Figure 3.2 a	Picture of column in vertical position	13
Figure 3.2 b	Vertical position of packed column	13
Figure 3.3 a	Picture of column in inclined position	14
Figure 3.3 b	Inclined position of packed column	14
Figure 4.1	Fitting of the partial mixing model and axial dispersion model to the experimental curve for probe 1 of the column in horizontal position with sand packing and a flow rate of 25 ml/min	21
Figure 4.2	Fitting of the partial mixing model and axial dispersion model to the experimental curve for probe 2 of the column in horizontal position with sand packing and a flow rate of 25 ml/min	23
Figure 4.3	Fitting of the partial mixing model and axial dispersion model to the experimental curve for probe 3 of the column in horizontal position with sand packing and a flow rate of 25 ml/min	25
Figure 4.4	Fitting of the partial mixing model and axial dispersion model to the experimental curve for probe 1 of the column in vertical position with sand packing and a flow rate of 25 ml/min	27
Figure 4.5	Fitting of the partial mixing model and axial dispersion model to the experimental curve for probe 2 of the column in vertical position with sand packing and a flow rate of 25 ml/min	29
Figure 4.6	Fitting of the partial mixing model and axial dispersion model to the experimental curve for probe 3 of the column in vertical position with sand packing and a flow rate of 25 ml/min	31

<u>FIGURE</u>	<u>TITLE</u>	<u>PAGE</u>
Figure 4.7	Fitting of the partial mixing model and axial dispersion model to the experimental curve for probe 1 of the column in inclined position with sand packing and a flow rate of 25 ml/min	33
Figure 4.8	Fitting of the partial mixing model and axial dispersion model to the experimental curve for probe 2 of the column in inclined position with sand packing and a flow rate of 25 ml/min	35
Figure 4.9	Fitting of the partial mixing model and axial dispersion model to the experimental curve for probe 3 of the column in inclined position with sand packing and a flow rate of 25 ml/min	37
Figure 4.10	Fitting of the partial mixing model and axial dispersion model to the experimental curve for probe 1 of the column in horizontal position with sand packing and a flow rate of 50 ml/min	39
Figure 4.11	Fitting of the partial mixing model and axial dispersion model to the experimental curve for probe 2 of the column in horizontal position with sand packing and a flow rate of 50 ml/min	41
Figure 4.12	Fitting of the partial mixing model and axial dispersion model to the experimental curve for probe 3 of the column in horizontal position with sand packing and a flow rate of 50 ml/min	43
Figure 4.13	Fitting of the partial mixing model and axial dispersion model to the experimental curve for probe 1 of the column in vertical position with sand packing and a flow rate of 50 ml/min	45
Figure 4.14	Fitting of the partial mixing model and axial dispersion model to the experimental curve for probe 2 of the column in vertical position with sand packing and a flow rate of 50 ml/min	4

<u>FIGURE</u>	<u>TITLE</u>	<u>PAGE</u>
Figure 4.15	Fitting of the partial mixing model and axial dispersion model to the experimental curve for probe 3 of the column in vertical position with sand packing and a flow rate of 50 ml/min	49
Figure 4.16	Fitting of the partial mixing model and axial dispersion model to the experimental curve for probe 1 of the column in inclined position with sand packing and a flow rate of 50 ml/min	51
Figure 4.17	Fitting of the partial mixing model and axial dispersion model to the experimental curve for probe 2 of the column in inclined position with sand packing and a flow rate of 50 ml/min	53
Figure 4.18	Fitting of the partial mixing model and axial dispersion model to the experimental curve for probe 3 of the column in inclined position with sand packing and a flow rate of 50 ml/min	55
Figure 4.19	Fitting of the partial mixing model and axial dispersion model to the experimental curve for probe 1 of the column in horizontal position with angular rock fragments packing and a flow rate of 25 ml/min	57
Figure 4.20	Fitting of the partial mixing model and axial dispersion model to the experimental curve for probe 2 of the column in horizontal position with angular rock fragments packing and a flow rate of 25 ml/min	59
Figure 4.21	Fitting of the partial mixing model and axial dispersion model to the experimental curve for probe 3 of the column in horizontal position with angular rock fragments packing and a flow rate of 25 ml/min	61
Figure 4.22	Fitting of the partial mixing model and axial dispersion model to the experimental curve for probe 1 of the column in vertical position with angular rock fragments packing and a flow rate of 25 ml/min	63

<u>FIGURE</u>	<u>TITLE</u>	<u>PAGE</u>
Figure 4.23	Fitting of the partial mixing model and axial dispersion model to the experimental curve for probe 2 of the column in vertical position with angular rock fragments packing and a flow rate of 25 ml/min	65
Figure 4.24	Fitting of the partial mixing model and axial dispersion model to the experimental curve for probe 3 of the column in vertical position with angular rock fragments packing and a flow rate of 25 ml/min	67
Figure 4.25	Fitting of the partial mixing model and axial dispersion model to the experimental curve for probe 1 of the column in inclined position with angular rock fragments packing and a flow rate of 25 ml/min	69
Figure 4.26	Fitting of the partial mixing model and axial dispersion model to the experimental curve for probe 2 of the column in inclined position with angular rock fragments packing and a flow rate of 25 ml/min	71
Figure 4.27	Fitting of the partial mixing model and axial dispersion model to the experimental curve for probe 3 of the column in inclined position with angular rock fragments packing and a flow rate of 25 ml/min	73
Figure 4.28	Fitting of the partial mixing model and axial dispersion model to the experimental curve for probe 1 of the column in horizontal position with angular rock fragments packing and a flow rate of 50 ml/min	75
Figure 4.29	Fitting of the partial mixing model and axial dispersion model to the experimental curve for probe 2 of the column in horizontal position with angular rock fragments packing and a flow rate of 50 ml/min	77
Figure 4.30	Fitting of the partial mixing model and axial dispersion model to the experimental curve for probe 3 of the column in horizontal position with angular rock fragments packing and a flow rate of 50 ml/min	79
Figure 4.31	Comparison between experimental and calculated efficiency and dispersion coefficient values as a function of probe position when column in horizontal position is packed with sand and at flow rates of 25 ml/min and 50 ml/min	98

<u>FIGURE</u>	<u>TITLE</u>	<u>PAGE</u>
Figure 4.31	Fitting of the partial mixing model and axial dispersion model to the experimental curve for probe 1 of the column in vertical position with angular rock fragments packing and a flow rate of 50 ml/min	81
Figure 4.32	Fitting of the partial mixing model and axial dispersion model to the experimental curve for probe 2 of the column in vertical position with angular rock fragments packing and a flow rate of 50 ml/min	83
Figure 4.33	Fitting of the partial mixing model and axial dispersion model to the experimental curve for probe 3 of the column in vertical position with angular rock fragments packing and a flow rate of 50 ml/min	85
Figure 4.34	Fitting of the partial mixing model and axial dispersion model to the experimental curve for probe 1 of the column in inclined position with angular rock fragments packing and a flow rate of 50 ml/min	87
Figure 4.35	Fitting of the partial mixing model and axial dispersion model to the experimental curve for probe 2 of the column in inclined position with angular rock fragments packing and a flow rate of 50 ml/min	89
Figure 4.36	Fitting of the partial mixing model and axial dispersion model to the experimental curve for probe 3 of the column in inclined position with angular rock fragments packing and a flow rate of 50 ml/min	91
Figure 4.37	Comparison between experimental and calculated residence times at flow rates of 25 ml/min and 50 ml/min using sand as packing material	96
Figure 4.38	Comparison between experimental and calculated residence times at flow rates of 25 ml/min and 50 ml/min using angular rock fragments as packing material	96
Figure 4.39	Variation of mixing efficiency and dispersion coefficient values as a function of probe position when column in horizontal position is packed with sand and at flow rates of 25 ml/min and 50 ml/min	98

<u>FIGURE</u>	<u>TITLE</u>	<u>PAGE</u>
Figure 4.40	Variation of mixing efficiency and dispersion coefficient values as a function of probe position when column in vertical position is packed with sand and at flow rates of 25 ml/min and 50 ml/min.	98
Figure 4.41	Variation of mixing efficiency and dispersion coefficient values as a function of probe position when column in inclined position is packed with sand and at flow rates of 25 ml/min and 50 ml/min.	99
Figure 4.42	Variation of mixing efficiency and dispersion coefficient values as a function of probe position when column in horizontal position is packed with angular rock fragments and at flow rates of 25 ml/min and 50 ml/min.	99
Figure 4.43	Variation of mixing efficiency and dispersion coefficient values as a function of probe position when column in vertical position is packed with angular rock fragments and at flow rates of 25 ml/min and 50 ml/min.	100
Figure 4.44	Variation of mixing efficiency and dispersion coefficient values as a function of probe position when column in inclined position is packed with angular rock fragments and at flow rates of 25 ml/min and 50 ml/min.	100

ACKNOWLEDGEMENTS

I would like to take this opportunity to express my appreciation and gratitude to all those who have helped me during this study. I sincerely wish to thank Dr. Isam Amin, my thesis advisor for his guidance, advice and support throughout this study. Working with him has always been interesting and rewarding. This thesis would have not have been possible if not for his support and guidance.

I sincerely wish to thank Dr. Douglas M. Price, my thesis co-advisor for providing valuable suggestions and support during the preparation of this document. I wish to thank Dr. Alan M. Jacobs, director of the Environmental Studies program and Mr. Scott C. Williams from the EPA for agreeing to serve on my thesis committee and providing useful and timely suggestions.

I wish to thank the University Research Council (URC) for funding this study, and the School of Graduate Studies, the department of Geological and Environmental Sciences and Dr. Charles Singler, chair of the department for providing the opportunity and financial support to pursue my graduate study here at Youngstown State University. Sincere thanks to Mr. Jerry Fullum and Mr. John Dodson for the construction of my experimental apparatus which was used in this study.

Special thanks to Ms. Rakshita Banwasi for providing support and for proof reading my thesis. I would now like to thank Dr. R. Parthasarathy and Mrs. Malathi Parthasarathy -my parents, Mrs. Pushpavalli Ragavan – my sister, Mr. S. Ragavan – my brother-in-law, and my niece R. Rupa who are the most important people in my life, for providing their unconditional love, affection, support and most of all for believing in me.

CHAPTER 1

1.0 INTRODUCTION

1.1 Groundwater residence time

Groundwater is the main source of water for human needs in many parts of the world including the United States of America. Rural Ohio is no exception. The abundance and the shallow depth of groundwater in Ohio especially in the northeastern part of the state, makes groundwater a reliable and attractive resource to utilize.

Major problems that affect groundwater resources are contamination and overdrafting. Groundwater contamination is caused mainly by anthropogenic sources and usually occurs in developed (industrial) countries. Overdrafting occurs when groundwater withdrawals significantly exceed the rate of groundwater recharge. Overdrafting causes permanent shortage of water, and can cause other geologic catastrophes such as land subsidence (sinking of the land), sinkhole formation and seawater intrusion in coastal aquifers.

Successful management of groundwater resources calls for the determination of the available volume of groundwater that can be withdrawn on a sustained basis (without overdraft). An efficient way to make this determination is to quantify the residence time of groundwater using natural or artificial tracers and mathematical models. Determination of the mean residence time by tracers is also very valuable in characterization and remediation of contaminated groundwater. In this case, the mean residence time can be used to calculate the average velocity of groundwater contaminants and the migration rate of the contaminant plume. Contaminant velocity determined by the physical (non-tracer)

approach is less accurate than those obtained by the mean residence time as the latter takes into account the effects of mixing patterns, which influence the contaminants concentrations, as will be explained later.

The amount, length or period of time spent by groundwater in aquifers between entry and exit points is called the groundwater residence time. Residence times vary widely from one area to the other in the aquifer depending on the hydraulic properties of the aquifer and the physical and chemical properties of groundwater.

1.2 Current tracer mathematical models

Current tracer mathematical models provide solutions to determine the mean residence time or transit time of groundwater in natural systems. The models describe the tracer input-output relationships for the system by means of the residence time distribution function also called the weighting function. Generally the weighting function is understood to be the tracer model (Maloszweski and Zuber, 1982). Tracer concentration is influenced by mixing due to hydrodynamic dispersion and molecular diffusion in natural groundwater systems. This effect is accounted for by assuming specific mixing fashion(s) in the development of the models (Amin, 1987).

“Perfect mixing” and “piston flow” are the two most commonly assumed mixing forms. Perfect mixing refers to the situation in which tracer concentration in the system is homogeneous and the output concentration is identical to that within the system (Himmelblau and Bischoff, 1968). Piston flow occurs when fluid velocity is uniform over the entire system and each element of fluid that enters the system “marches” without intermingling with the other fluid elements that entered earlier or later (Himmelblau and

Bischoff, 1968). Piston flow describes the case of no mixing, meaning little or no dispersion in the system. Both perfect mixing and piston flow represent limiting extreme cases that seldom occur in groundwater systems or other natural hydrologic systems (Amin, 1987).

In most cases of natural groundwater flow systems, the form of mixing that takes place lies somewhere in between the two extremes of perfect mixing and no mixing (piston flow). This type of mixing is called partial mixing, as opposed to perfect or complete mixing, and the model that simulates it is called the partial mixing model (Amin, 1987).

1.3 Statement of the problem

Current groundwater tracer models are based on theoretical considerations that are not subjected to experimental verification. Many theoretical tracer models are currently used to calculate the residence times of groundwater in aquifers. These theoretical models have not been experimentally verified prior to their application in field studies. Therefore, the suitability of these tracer models to even simple laboratory-controlled conditions is not known due to lack of prior experimental verification.

1.4 Objective

The overall objective of this research is the experimental verification of the partial mixing model. The proposed verification will show the extent to which the model is suitable or applicable to simple laboratory conditions and ultimately the complex natural

systems of groundwater. The objective is achieved using packed columns in the laboratory, as will be explained in Chapter 3.

2.1 Lumped parameter models

The simplest common approach used in the interpretation of tracer data in hydrologic systems is the lumped parameter or the "black box" approach (Zuber, 1981).

The use of tracers to estimate hydrologic system parameters is based on mathematical models which describe the input-output relationships for the system, as explained earlier. The use of mathematical models requires a thorough understanding of the system's internal structure and the physical processes relating to the input and output of the system. These processes and the internal structure of groundwater systems are often simplified due to limitations pertaining to available data. Therefore, in the lumped parameter approach spatial variations are ignored, and are commonly simplified by lumping or spatially averaging the input, output (system response), and the system parameters (Amin, 1987).

One of the most essential parameters to be obtained from the lumped parameter approach is the mean residence time or the true residence time of the hydrologic system. In some cases, the approach also allows determination of other parameters that define the system. The lumped parameter approach is particularly useful in interpreting tracer data variable in time; however, it does not give an unequivocal answer for systems with constant tracer input unless some physical knowledge of the system is available (Zuber, 1981).

CHAPTER 2

2.0 LITERATURE REVIEW AND THEORETICAL BACKGROUND

2.1 Lumped parameter models

The most common approach used in the interpretation of tracer data in hydrologic systems is the lumped parameter or the “black box” approach (Zuber, 1986).

The use of tracers to estimate hydrologic systems parameters is based on mathematical models which describe the tracer input-output relationships for the system, as explained earlier. The use of mathematical models requires a thorough understanding of the system's internal structure and the physical processes relating to the input and output of the system. These processes and the internal structure of groundwater systems are often simplified due to limitations pertaining to available data. Therefore, in the lumped parameter approach spatial variations are ignored, and are commonly simplified by lumping or spatially averaging the input, output (system response), and the system parameters (Amin, 1987).

One of the most essential parameters to be obtained from the lumped parameter approach is the mean transit time or the mean residence time of the hydrologic system. In some cases, the approach also allows determination of other parameters that define the system. The lumped parameter approach is particularly useful in interpreting tracer data variable in time; however, it does not give an unequivocal answer for systems with constant tracer input unless some physical knowledge of the system is available (Zuber, 1985).

Lumped parameter models that are often used in the interpretation of environmental tracer data in groundwater systems are the piston flow model, exponential or perfect mixing model, linear model, exponential piston flow model, linear piston flow model, dispersive models, partial mixing model, and discrete state compartment models. The later can be considered as distributed parameter models with lumping if prior knowledge of the system exists (Maloszweski and Zuber, 1982).

Radioactive isotopes are often used as tracers. The piston flow model assumes that the concentration of a tracer changes only due to radioactive decay. Thus, it applies only to cases where little or no mixing occurs in the groundwater system. The exponential model was introduced by Eriksson (1958) under the assumption that the exponential distribution of transit times corresponds to a probable situation of decreasing permeability with the aquifer depth. The linear model describes an aquifer with linearly increasing thickness and a constant hydraulic gradient. When the linear model is combined with the piston flow model, it gives the linear piston flow model (Maloszweski and Zuber, 1982).

The dispersive models are obtained from the solution of the unidimensional form of the dispersion equation. Four analytical solutions are possible depending on the boundary conditions which describe the injection-detection mode of the tracer (Maloszweski and Zuber, 1982). Discrete state compartment models are mixing cell models. In these models, the system is divided into mixing cells which can be of any size, and may be arranged on one-, two-, or three-dimensional networks. Determination of tracer output concentration is made by specifying the mixing type and applying the conservation of mass to each cell (Maloszweski and Zuber, 1982). The partial mixing

model follows the three-parameter gamma distribution, and simulates mixing using the mixing efficiency, a parameter that varies from zero for no mixing (piston flow) to 1 for complete (perfect) mixing (Amin, 1987; Amin and Campana, 1996).

Currently, partial mixing is modeled by the dispersive models (Nir, 1964; Maloszweski and Zuber, 1982), discrete-state compartment models (Przewlocki and Yurtsever, 1974; Campana, 1975; Simpson and Duckstein, 1976), and the partial mixing model. The dispersive models and discrete-state compartment models have certain limitations. The dispersive model is limited to one-dimensional flow systems (Amin, 1987). The dispersivity is scale-dependant and hence difficult to estimate. Furthermore, the use of dispersive models in its lumped parameter form is not theoretically justified for systems other than packed beds or pipelines with turbulent or laminar flow including rivers and karstic conduits (Zuber, 1986). In groundwater systems, it is assumed that injection takes place at a point, whereas it actually extends over the recharge area (Zuber, 1985). Therefore, the dispersivity observed in the lumped parameter approach as applied to environmental tracers is an apparent one and has nothing to do with real dispersion processes (Zuber, 1985). Discrete-state compartment models, on the other hand, are convenient for modeling spatial variations of the parameters (i.e., they should be treated as distributed parameter models), but they are unsuitable for solving the inverse problem because of their large number of fitting parameters (Zuber, 1986). The partial mixing model, the subject of experimental verification in this study, is free from the limitations of the dispersive models and discrete-state compartment models (Amin, 1987; Amin and Campana 1996).

2.2 Models and their hydrogeological significance

Different tracer models apply to different types of aquifers. The major types of aquifers are confined, semi-confined and unconfined aquifers. Aquifers may have constant or variable thickness. Due to the varying nature of aquifers and their thickness, only certain tracer models apply to specific aquifers. For example, the piston flow model (no mixing) and the partial mixing model with a low mixing efficiency apply to a confined aquifer with a narrow recharge area far from the sampling wells; the exponential model and the partial mixing model with high mixing efficiency apply to an unconfined aquifer with the exponential distribution of transit times and also apply to an aquifer partly confined; the linear model is applicable to an unconfined aquifer with a gradual increase in its thickness; and the linear and the piston flow models are applicable to aquifers with increasing thickness that are partly confined (Maloszewski and Zuber, 1982).

2.3 Determination of the mean transit time by the lumped parameter approach

As mentioned earlier, the mean residence time is the most essential parameter to be obtained from lumped parameter models using tracer data. The mean residence time is of great importance because it leads to the evaluation of other crucial parameters such as total volume of mobile water and the average effective porosity of the groundwater system (Amin, 1987). The total volume of mobile water (V_T), which is the water accessible to the tracer in the system, is determined from Equation (1) below if the mean residence time (T) and the volumetric flow rate (Q) through the system are known.

$$T = \frac{V_T}{Q} \quad (1)$$

Quantitative interpretation of tracer data is particularly useful in investigating systems which lack detailed hydrologic data and systems where the traditional (physical, non tracer) hydrologic methods do not give satisfactory results, such as karst formations or fractured systems (Zuber, 1986). Little or no groundwater data is available in developing countries. In these countries the use of tracer data can be the only tool available for evaluation of groundwater resources (Amin, 1987). As indicated in Chapter 1, tracers can provide valuable information regarding the characterization and remediation of contaminated groundwater systems in developed (industrial) countries, such as the nature and degree of mixing, which influence the concentration of contaminants, and the average velocity of contaminants.

In order to evaluate the mean residence time, the proper tracer model that best describes mixing in the groundwater system should be used. This model should be able to relate the input and output concentrations. Theoretical curves which represent the “calculated” tracer output concentrations obtained from the model are made to fit experimental curves, which represent the “measured” tracer output concentrations, to determine the mean residence time. This is the reason why the choice of the proper tracer model is very important. There are two different situations when dealing with the input to the system. The tracer input can be constant or variable with steady or transient flow. In the case of variable input to the system, the mean residence time is determined by the best fit of calculated and observed graphs of output concentrations, as explained above. Analytical evaluation of the mean residence time in the case of constant input and steady flow requires no additional information if the selected model is a one-parameter model, such as the piston flow or the perfect mixing model. For two or more parameter models,

prior knowledge of the parameters other than the mean residence time, the unknown, is necessary (Zuber, 1986). Therefore, it can be seen that tracers with variable inputs are more flexible and offer better opportunities to determine the mean residence time than those with constant inputs (Amin, 1987; Maloszewski and Zuber, 1982).

2.4 Partial mixing

As described earlier, partial mixing is defined as the type of mixing pattern observed in natural groundwater flow, which takes place somewhere in between piston flow and perfect mixing. Piston flow and perfect mixing are the two extremes of mixing. Piston flow indicates zero or no mixing and perfect mixing indicates complete mixing, as opposed to partial mixing. In other words piston flow patterns represent the lower limit of the mixing range and perfect mixing patterns represent the upper limit. Partial mixing is better described as the type of mixing which can range from near perfect mixing (upper limit) to near piston flow (lower limit), but never reaches these extremes (Amin, 1987). Instead of describing the partial mixing pattern as somewhere in between piston flow and perfect mixing, it would be ideal to be able to exactly pin-point its location or level of mixing. For this purpose, the concept of mixing efficiency is introduced by Amin (1987).

In hydrologic systems, mixing is due to hydrodynamic dispersion and molecular diffusion. The partial mixing model, like all other lumped parameter models, is applicable to systems in which molecular diffusion is negligible. In other words the mixing efficiency, μ , is defined as a lumped parameter that describes mixing due to hydrodynamic dispersion (Amin, 1987). The value of the mixing efficiency describes the location or extent of partial mixing taking place in the system as follows:

$\mu = 1$ for perfect mixing; 0 for piston flow and somewhere in between 0 and 1 ($0 < \mu < 1$) for partial mixing. As explained earlier, the partial mixing model employs the mixing efficiency (μ) to simulate mixing and determine the mean residence time (T) of the hydrologic system.

Experimental verification of the partial mixing model was carried out in the laboratory by simulating the flow of natural groundwater using a column packed with sand and later with angular rock fragments. Water was passed through the column from one end to the other at a controlled flow rate, and, an aqueous solution of sodium chloride (NaCl) was used as a tracer to investigate mixing patterns in the column. The concentration of sodium chloride in the column was acquired as electrical conductivity values using four conductivity probes inserted at different locations along the column length.

Experimental verification of the partial mixing model was conducted for three types groundwater flow: horizontal flow, vertical flow, and flow with both vertical and horizontal components. These three flow types were simulated by orienting the packed column in the horizontal, vertical and inclined positions respectively, as shown in Figures 3.1 (a,b), 3.2 (a,b) and 3.3 (a,b).



Figure 3.1 (a) Picture of column in the horizontal position

CHAPTER 3

3.0 METHODS AND PROCEDURES

3.1 Introduction

Experimental verification of the partial mixing model was carried out in the laboratory by simulating the flow of natural groundwater using a column packed with sand and later with angular rock fragments. Water was passed through the column from one end to the other at a controlled flow rate, and an aqueous solution of sodium chloride (NaCl) was used as a tracer to investigate mixing patterns in the column. The concentration of sodium chloride in the column was acquired as electrical conductivity values using four conductivity probes inserted at different locations along the column length.

Experimental verification of the partial mixing model was conducted for three types groundwater flow: horizontal flow, vertical flow, and flow with both vertical and horizontal components. These three flow types were simulated by orienting the packed column in the horizontal, vertical and inclined positions respectively, as shown in Figures 3.1 (a,b), 3.2 (a,b) and 3.3 (a,b).

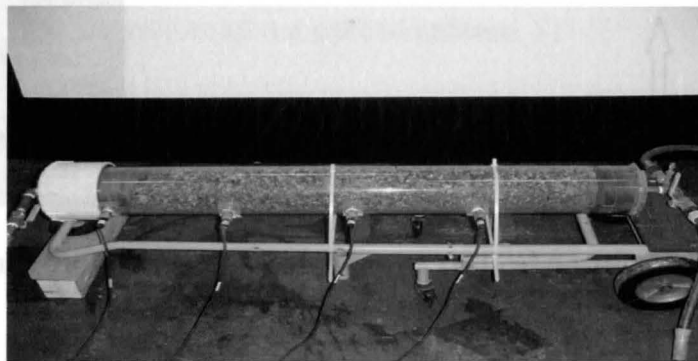


Figure 3.1 (a): Picture of column in the horizontal position

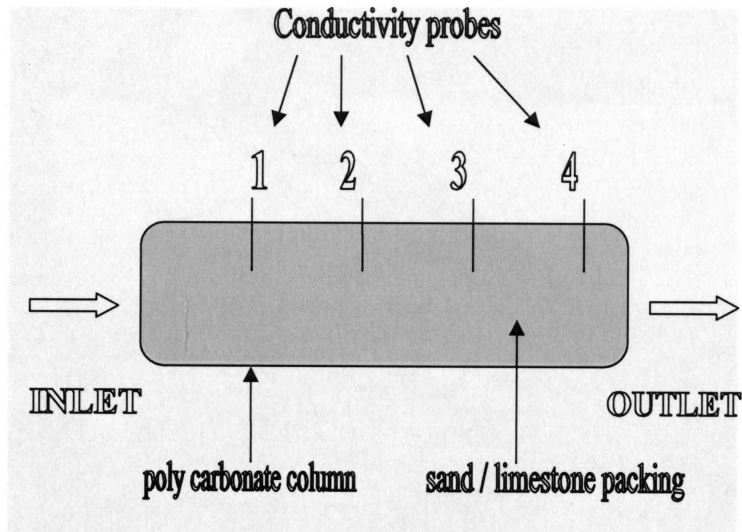


Figure 3. 1 (b): Horizontal position of the packed column

Figure 3.3 (a): Picture of column in the inclined position

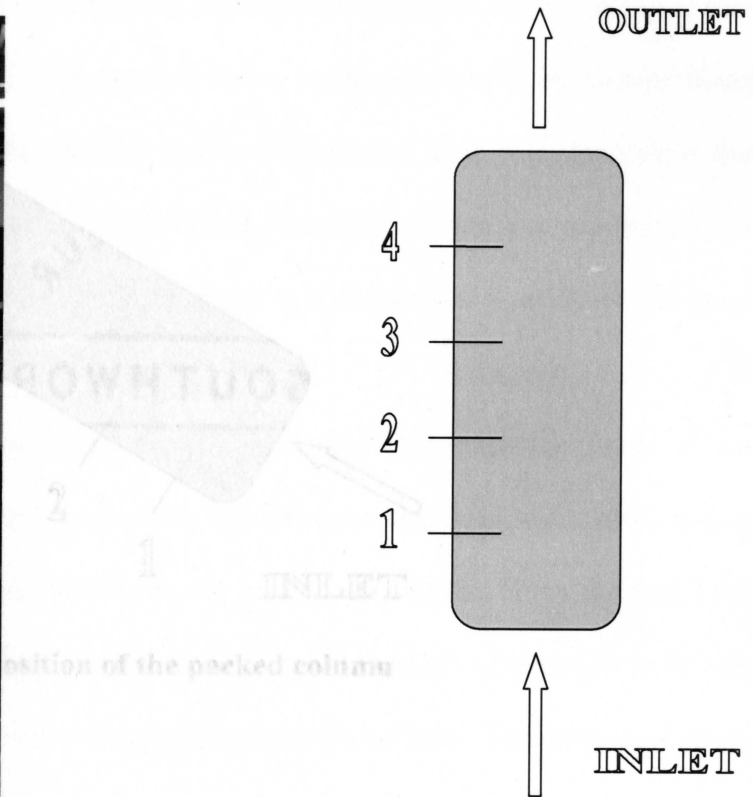
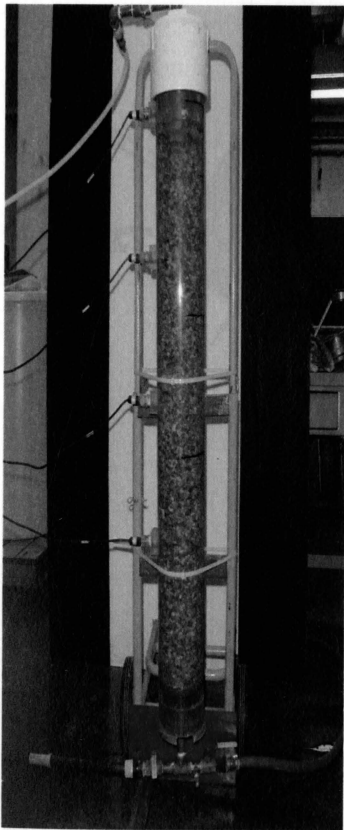


Figure 3.2 (a) and (b): Picture of column in the vertical position; vertical position of the packed column.

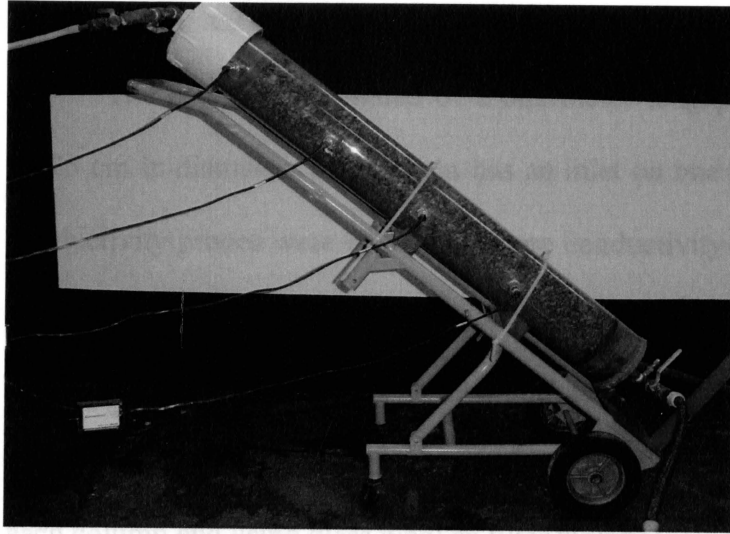


Figure 3.3 (a): Picture of column in the inclined position

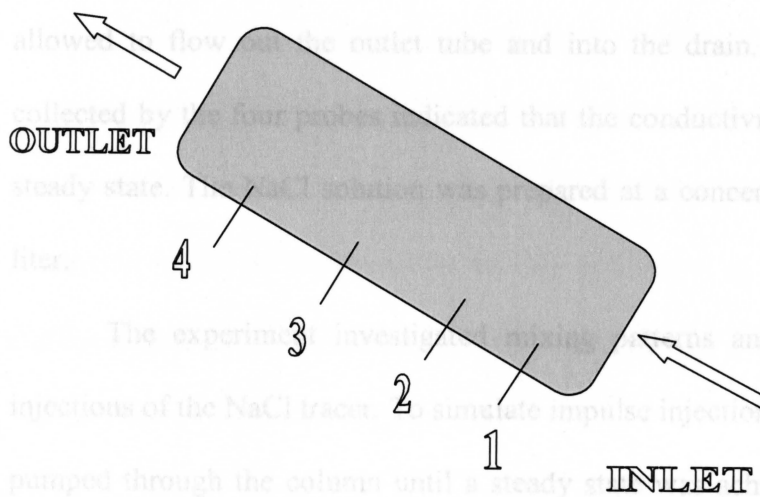


Figure 3.3 (b): Inclined position of the packed column

3.2 Experimental apparatus

The apparatus consisted of a one meter long poly-carbonate column measuring 15.25 cm in diameter. The column has an inlet on one end and outlet on the other. Four conductivity probes were used to measure conductivity in $\mu\text{S}/\text{cm}$ at various points in the column. The four probes were inserted at equal intervals from each other along the length of the column. The column was then packed with sand to a level just below that of the last probe closest to the outlet. The packed sand was held in place using screens placed at each column end using glass wool as filter material.

The column was then filled with city water through the inlet. The initial set-up of the apparatus was vertical, with the inlet at the bottom and outlet at the top. Water was allowed to flow out the outlet tube and into the drain. This was done until the data collected by the four probes indicated that the conductivity measurements have reached steady state. The NaCl solution was prepared at a concentration of about six grams per liter.

The experiment investigated mixing patterns and residence times of impulse injections of the NaCl tracer. To simulate impulse injection, fresh water was continuously pumped through the column until a steady state was achieved. Then the NaCl solution was allowed to flow through the column for a certain amount of time (30 to 40 minutes) and then once again fresh water was pumped in to the column. This procedure developed sharp conductivity peaks resulting from the contact of NaCl solution with the four probes. The conductivity data was collected at 0.1 minute intervals by computer data acquisition. Thus, the experiment plots four different curves/peaks representing each of the four probes in the column.

3.3 Impulse tracer injection - The partial mixing model

The experiment run was completed when steady state was once again reached after developing a peak. This steady state indicated that NaCl solution has passed the column and that the column is once again filled with fresh water. Using the conductivity readings recorded by the four conductivity probes, a graph was plotted using excel with $C(t)$ values on the y-axis and running time on the x-axis. This curve represented the experimental curve, and was a reflection of the behavior of a tubular reactor subjected to impulse tracer injection.

The tracer models investigated for the purpose of impulse injection reactions employ a new parameter – the mixing efficiency, for simulating mixing and determining the residence times in groundwater systems. In this study, the partial mixing model employs mixing efficiency and the mean residence time as the fitting parameter. The purpose of this research is to experimentally verify the partial mixing model and the axial dispersion model to determine the mixing efficiency, μ , the dispersion coefficient, D_L and the mean residence time for flow patterns observed in the column.

The partial mixing model is given by;

$$G(t) = \frac{\left(t - T\left(1 - \frac{1}{\alpha}\right)\right)^{(\alpha-1)}}{\left(\frac{T}{\alpha^2}\right)^\alpha \Gamma(\alpha)} * \exp\left(-\frac{t - T\left(1 - \frac{1}{\alpha}\right)}{\left(\frac{T}{\alpha^2}\right)}\right) \quad (2)$$

Where, $G(t)$ is the system response function, t is the running time, T is the mean residence time $\alpha = 1/\mu$; $\mu =$ mixing efficiency; $\Gamma(\alpha) =$ gamma function of α ($\alpha = 1/\mu$).

The axial dispersion model for an impulse injection of tracer concentration as given by Hill (1977) is as follows:

$$C(t) = \int_0^\infty C(t) dt \frac{1}{2\sqrt{\pi \frac{D_L t}{uL}}} \exp \frac{-\left(1 - \left(\frac{t}{t^*}\right)\right)^2}{\left(\frac{4D_L}{uL}\right)\left(\frac{t}{t^*}\right)} \quad (3)$$

Where, D_L is the dispersion coefficient, t is the time after injection, $t^* = L/u$, u is the velocity of the fluid.

$$u = \frac{Q}{\varepsilon * A} \quad (4)$$

In the same manner as mentioned earlier, $C(t)$ values obtained from the column were used to plot experimental curves. The next step was calculating $G(t)$ values using Equation (2). For this purpose, the mixing efficiency, μ and the mean residence time, T were assumed and a set of values for $G(t)$ was generated in excel. Two graphs were plotted one using the set of $C(t)$ values on the y-axis and t on the x-axis as mentioned earlier, and the other, which represented the model curve, using $G(t)$ values on the y-axis and t on the x-axis. The goal was to determine the best fit of these two curves. Fitting yielded the specific mixing efficiency, μ and the mean residence time, T using the partial mixing model.

Using the same procedure, $C(t)$ model values were generated assuming an initial value for the dispersion coefficient, D_L and the mean residence time. A graph was plotted with the experimental data on the y – axis and calendar time, t on the x – axis. A second graph was plotted with the $C(t)$ model values on the y – axis and time, t on the x – axis. The goal was to determine the best fit of these two curves. Fitting will yield the

dispersion coefficient, D_L and the mean residence time, t^* using the axial dispersion model.

The flow patterns were observed using a column packed with sand. The next phase was to replace sand in the column with angular rock fragments, which was sieved using an opening of 2.83 mm or 0.111 inches. The sand (porosity 0.4) in the column was removed and angular rock fragments were added. The same set of experiments were repeated and recorded. Horizontal, vertical and inclined (20 to 25 degrees with ground level) pulse injection of tracer concentrations in angular rock fragments media was observed and modeled using the partial mixing model.

Results of each experimental run consist of time and conductivity obtained from the lower three probes. The results are presented in tabular and graphical forms. Conductivity measurements were taken every tenth of a minute. The tables, however, show only representative conductivity values.

The experimental data (conductivity values) from the three probes were fitted to the partial mixing model and the axial dispersion model. Each model used two fitting parameters: the partial mixing model used the mean residence time and the mixing efficiency, and the axial dispersion model used the mean residence time and the dispersion coefficient. In other words, the mixing efficiency, the dispersion coefficient, and the mean residence time were determined as fitting parameters.

Fitting was achieved by comparing the "experimental" curves of conductivity values with those "calculated" by the partial mixing model and those "calculated" by the axial dispersion model. The calculated conductivity values were obtained using the solver tool in Microsoft Excel, version 3.0, which minimizes the errors (differences

CHAPTER 4

4.0 RESULTS AND DISCUSSIONS

4.1 Introduction

This chapter summarizes the results of the experimental verification of the partial mixing model. As explained earlier, experimental runs were made for three column positions: horizontal, vertical, and inclined (20 – 25 degrees with ground level). In each run, the column was packed with either sand or angular rock fragments. Results of each experimental run consist of time and conductivity obtained from the lower three probes. The results are presented in tabular and graphical forms. Conductivity measurements were taken every tenth of a minute. The tables, however, show only representative conductivity values.

The experimental data (conductivity values) from the three probes were fitted to the partial mixing model and the axial dispersion model. Each model used two fitting parameters: the partial mixing model used the mean residence time and the mixing efficiency, and the axial dispersion model used the mean residence time and the dispersion coefficient. In other words, the mixing efficiency, the dispersion coefficient, and the mean residence time were determined as fitting parameters.

Fitting was achieved by comparing the “experimental” curves of conductivity values with those “calculated” by the partial mixing model and those “calculated” by the axial dispersion model. The calculated conductivity values were obtained using the solver tool in Microsoft Excel, version 3.0, which minimizes the errors (differences

between the experimental and calculated values). The figures shown below represent the best fit (the fit with minimum errors) of the experimental and calculated values.

4.2 The experimental runs

4.2.1 Horizontal position with sand packing – Flow rate: 25 ml/min

This experimental run was performed with a flow rate of 25 ml/min. Results for each of the three probes are given below.

Table 4.1: Horizontal position with sand packing – flow rate: 25 ml/min (probe 1).

Fitting yielded a mixing efficiency of 0.342, a dispersion coefficient of $0.36 \text{ cm}^2/\text{sec}$ and a mean residence time of 95.23 min.

Time, t (min)	Conductivity, C(t) ($\mu\text{S}/\text{cm}$)
1	114.564
5	114.564
10	95.470
20	114.564
30	105.017
40	95.470
50	257.769
60	1966.681
70	2014.422
80	2014.423
90	2052.612

Time, t (min)	Conductivity, C(t) ($\mu\text{S}/\text{cm}$)
100	3083.681
150	295.955

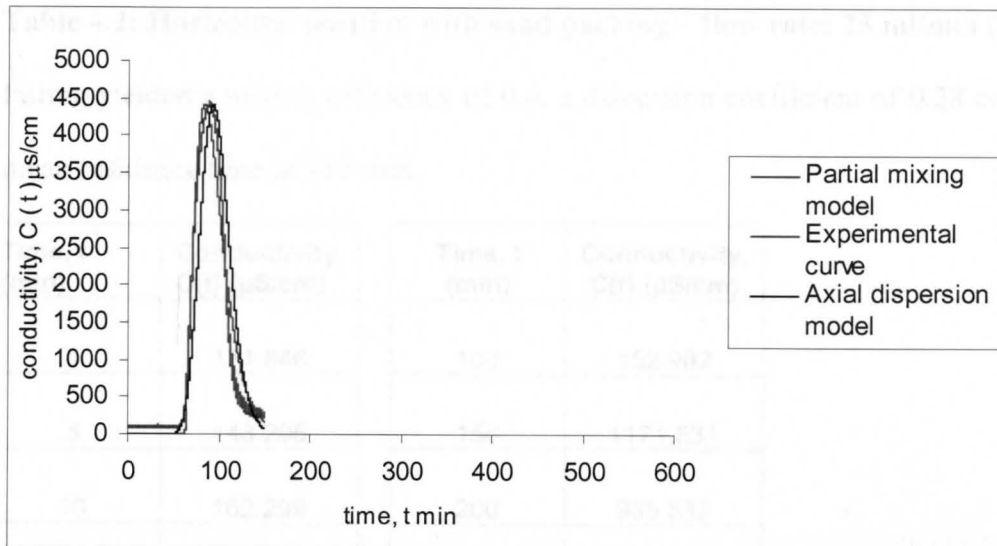


Figure 4.1: Fitting of the partial mixing model and axial dispersion model to the experimental curve for probe 1 of the column in horizontal position with sand packing and a flow rate of 25 ml/min.

Table 4.2: Horizontal position with sand packing – flow rate: 25 ml/min (probe 2).

Fitting yielded a mixing efficiency of 0.4, a dispersion coefficient of $0.28 \text{ cm}^2/\text{sec}$ and a mean residence time of 185 min.

Time, t (min)	Conductivity, C(t) ($\mu\text{S}/\text{cm}$)	Time, t (min)	Conductivity, C(t) ($\mu\text{S}/\text{cm}$)
1	171.846	100	152.982
5	143.205	150	1171.531
10	162.299	200	935.532
20	162.299	250	286.795
30	162.299	300	200.393
40	171.846	350	162.299
50	162.299	400	133.658
60	133.752		
70	162.752		
80	142.752		
90	181.846		

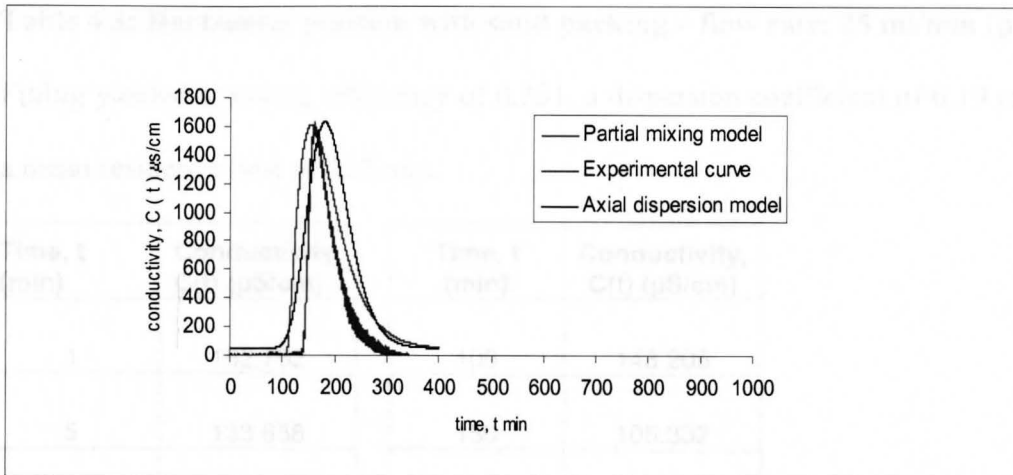


Figure 4.2: Fitting of the partial mixing model and the axial dispersion model to the experimental curve for probe 2 of the column in horizontal position with sand packing and a flow rate of 25 ml/min.

Table 4.3: Horizontal position with sand packing – flow rate: 25 ml/min (probe 3).

Fitting yielded a mixing efficiency of 0.351, a dispersion coefficient of 0.19 cm²/sec and a mean residence time of 255 min.

Time, t (min)	Conductivity, C(t) (μS/cm)
1	152.752
5	133.658
10	143.205
20	114.658
30	112.752
40	123.205
50	123.658
60	113.658
70	143.658
80	124.111
90	133.658

Time, t (min)	Conductivity, C(t) (μS/cm)
100	143.205
150	105.332
200	114.241
250	1460.791
300	591.241
350	257.957
400	162.294

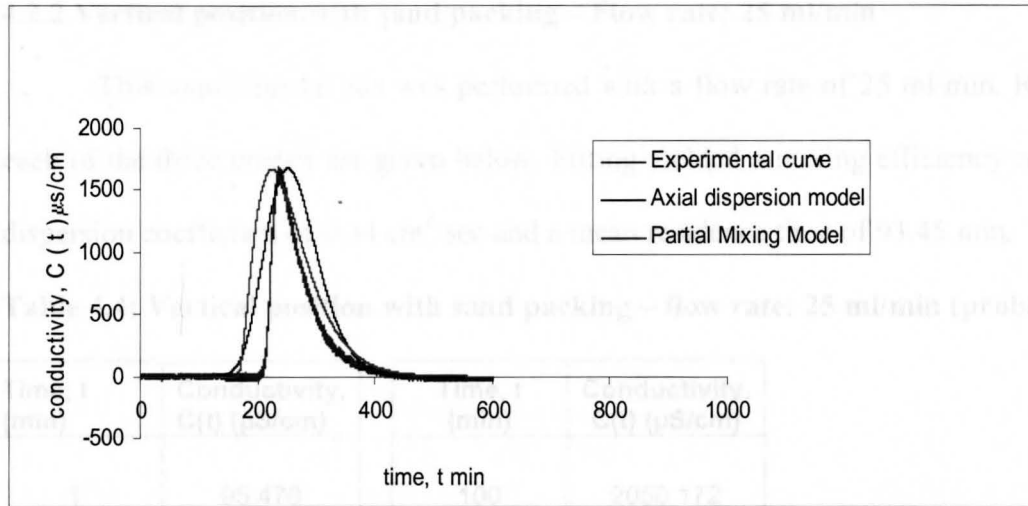


Figure 4.3: Fitting of the partial mixing model and the axial dispersion model to the experimental curve for probe 3 of the column in horizontal position with sand packing and a flow rate of 25 ml/min.

10	
20	
30	85 475
40	105 017
50	105 222
60	105 675
70	387 128
80	4506 982
90	3798 713

4.2.2 Vertical position with sand packing – Flow rate: 25 ml/min

This experimental run was performed with a flow rate of 25 ml/min. Results for each of the three probes are given below. Fitting yielded a mixing efficiency of 0.335, a dispersion coefficient of $0.34 \text{ cm}^2/\text{sec}$ and a mean residence time of 93.45 min.

Table 4.4: Vertical position with sand packing – flow rate: 25 ml/min (probe 1).

Time, t (min)	Conductivity, C(t) ($\mu\text{S}/\text{cm}$)
1	95.470
5	95.470
10	95.470
20	95.470
30	95.470
40	105.017
50	105.222
60	105.675
70	391.128
80	4506.992
90	3799.713

Time, t (min)	Conductivity, C(t) ($\mu\text{S}/\text{cm}$)
100	2050.172
150	243.204

Figure 4.4: Fitting of the partial mixing model and axial dispersion model to the experimental curve for probe 1 of the column in vertical position with sand packing and a flow rate of 25 ml/min.

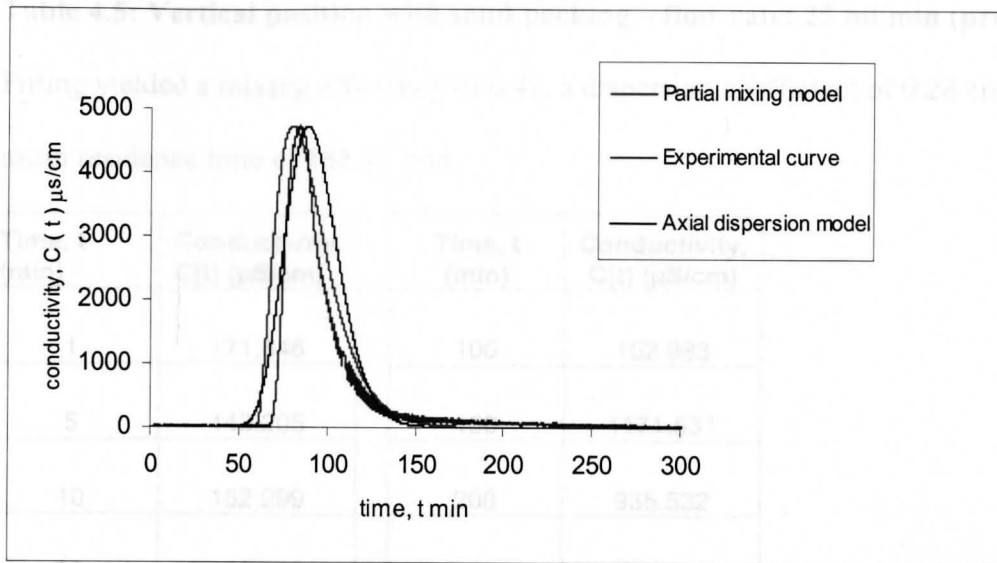


Figure 4.4: Fitting of the partial mixing model and axial dispersion model to the experimental curve for probe 1 of the column in vertical position with sand packing and a flow rate of 25 ml/min.

Table 4.5: Vertical position with sand packing – flow rate: 25 ml/min (probe 2).

Fitting yielded a mixing efficiency of 0.41, a dispersion coefficient of $0.28 \text{ cm}^2/\text{sec}$ and a mean residence time of 185.33 min.

Time, t (min)	Conductivity, C(t) ($\mu\text{S}/\text{cm}$)	Time, t (min)	Conductivity, C(t) ($\mu\text{S}/\text{cm}$)
1	171.846	100	152.983
5	143.205	150	1171.531
10	162.299	200	935.532
20	162.299	250	286.795
30	162.299	300	200.393
40	171.846	350	162.299
50	162.299	400	133.658
60	133.752		
70	162.752		
80	142.752		
90	181.846		

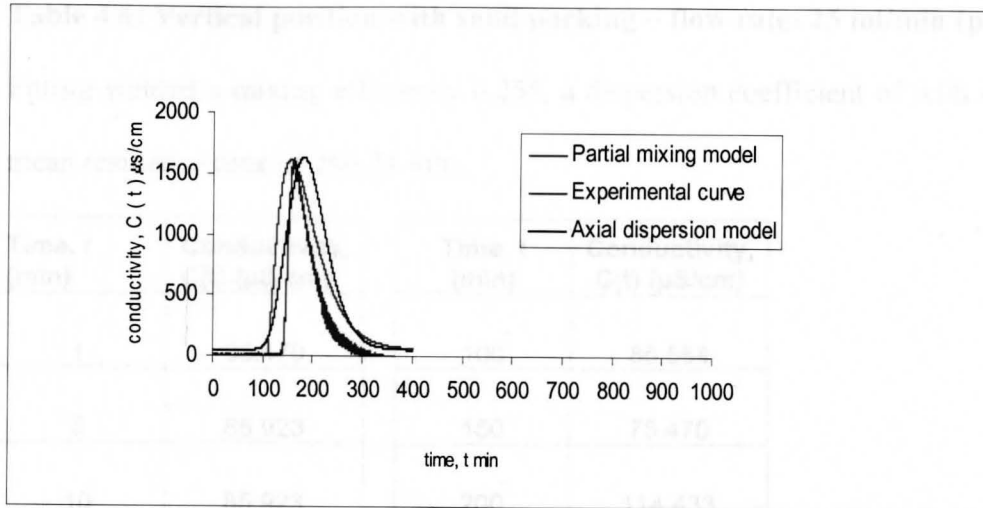


Figure 4.5: Fitting of the partial mixing model and the axial dispersion model to the experimental curve for probe 2 of the column in the vertical position with sand packing and a flow rate of 25 ml/min.

Table 4.6: Vertical position with sand packing – flow rate: 25 ml/min (probe 3).

Fitting yielded a mixing efficiency 0.255, a dispersion coefficient of $0.08 \text{ cm}^2/\text{sec}$ and a mean residence time of 260.24 min.

Time, t (min)	Conductivity, C(t) ($\mu\text{S}/\text{cm}$)
1	95.470
5	85.923
10	85.923
20	76.376
30	95.470
40	85.923
50	95.470
60	114.564
70	105.017
80	95.470
90	85.923

Time, t (min)	Conductivity, C(t) ($\mu\text{S}/\text{cm}$)
100	85.564
150	75.470
200	114.433
250	1116.962
300	792.411
400	286.487

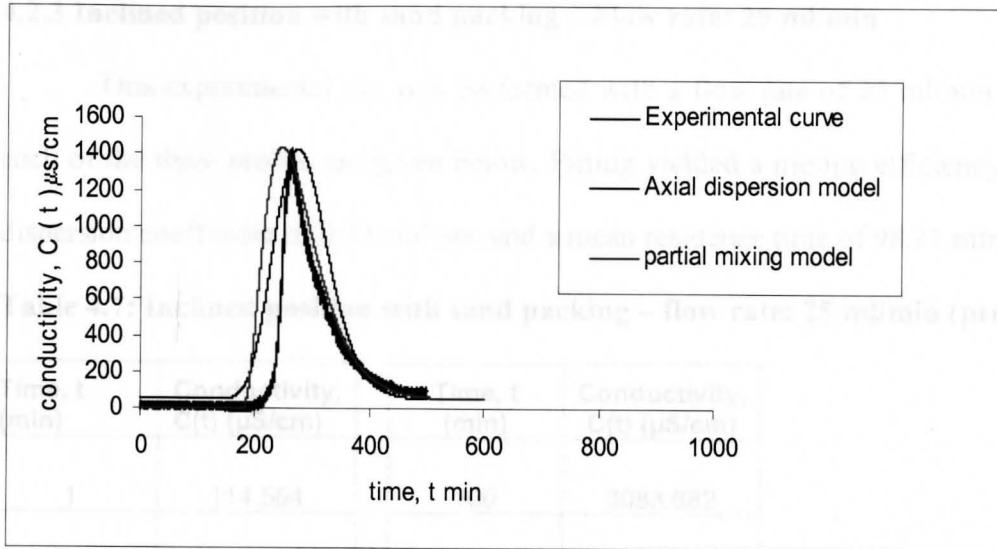


Figure 4.6: Fitting of the partial mixing curve and the axial dispersion curve to the experimental curve for probe 3 of the column in the vertical position with sand packing and a flow rate of 25 ml/min.

4.2.3 Inclined position with sand packing – Flow rate: 25 ml/min

This experimental run was performed with a flow rate of 25 ml/min. Results for each of the three probes are given below. Fitting yielded a mixing efficiency of 0.342, a dispersion coefficient of $0.33 \text{ cm}^2/\text{sec}$ and a mean residence time of 98.21 min.

Table 4.7: Inclined position with sand packing – flow rate: 25 ml/min (probe 1).

Time, t (min)	Conductivity, C(t) ($\mu\text{S}/\text{cm}$)	Time, t (min)	Conductivity, C(t) ($\mu\text{S}/\text{cm}$)
1	114.564	100	3083.682
5	114.564	150	295.951
10	95.470		
20	114.564		
30	105.017		
40	95.470		
50	257.769		
60	1966.682		
70	2014.421		
80	2014.422		
90	2052.611		

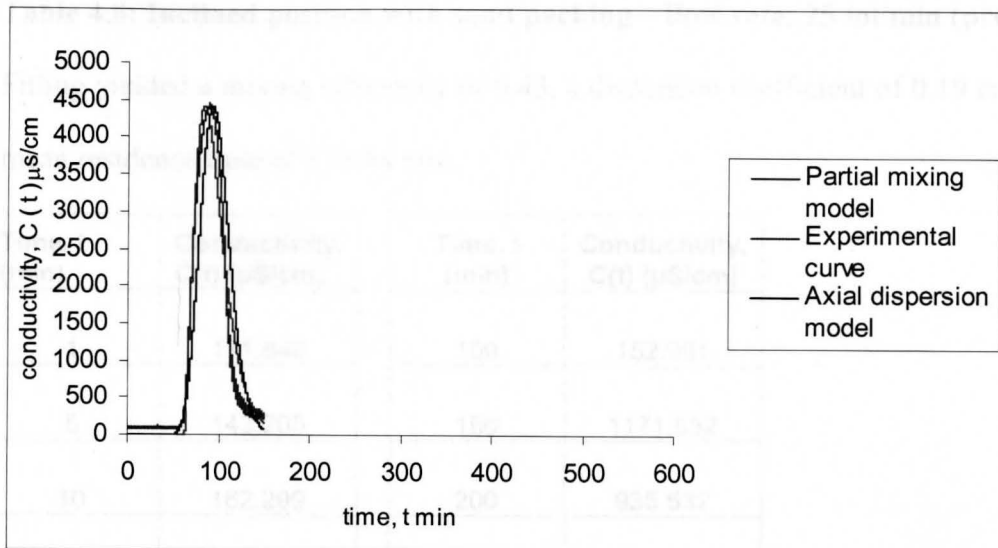


Figure 4.7: Fitting of the partial mixing model and the axial dispersion model to the experimental curve for probe 1 of the column in the inclined position with sand packing and a flow rate of 25 ml/min.

Table 4.8: Inclined position with sand packing – flow rate: 25 ml/min (probe 2).

Fitting yielded a mixing efficiency of 0.43, a dispersion coefficient of $0.19 \text{ cm}^2/\text{sec}$ and a mean residence time of 170.44 min.

Time, t (min)	Conductivity, C(t) ($\mu\text{S}/\text{cm}$)
1	171.846
5	143.205
10	162.299
20	162.299
30	162.299
40	171.846
50	162.299
60	133.752
70	162.752
80	142.752
90	181.846

Time, t (min)	Conductivity, C(t) ($\mu\text{S}/\text{cm}$)
100	152.981
150	1171.532
200	935.532
250	286.795
300	200.393
350	162.299
400	133.658

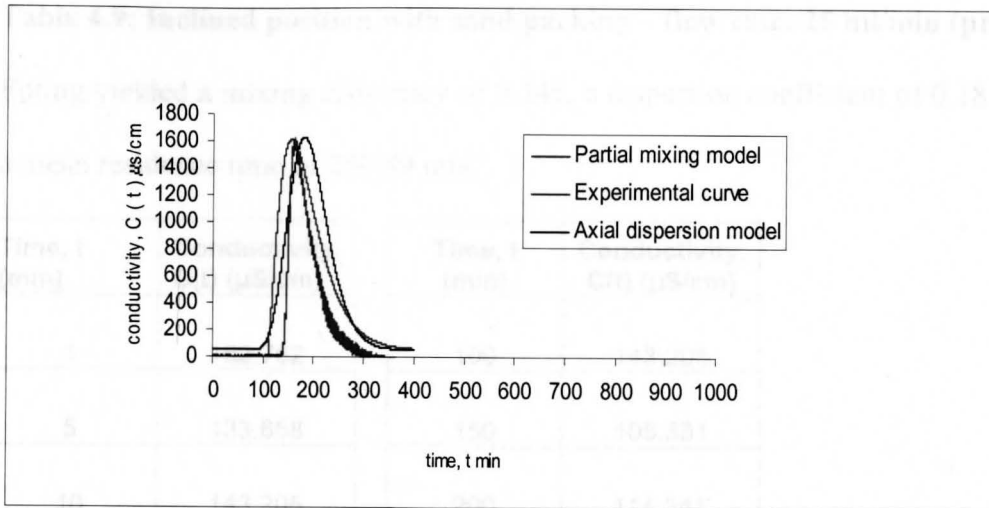


Figure 4.8: Fitting of the partial mixing model and the axial dispersion model to the experimental for probe 2 of the column in the inclined position with sand packing and a flow rate of 25 ml/min.

Table 4.9: Inclined position with sand packing – flow rate: 25 ml/min (probe 3).

Fitting yielded a mixing efficiency of 0.345, a dispersion coefficient of $0.18 \text{ cm}^2/\text{sec}$ and a mean residence time of 250.89 min.

Time, t (min)	Conductivity, C(t) ($\mu\text{S}/\text{cm}$)
1	152.752
5	133.658
10	143.205
20	114.658
30	112.752
40	123.205
50	123.658
60	113.658
70	143.658
80	124.111
90	133.658

Time, t (min)	Conductivity, C(t) ($\mu\text{S}/\text{cm}$)
100	143.205
150	105.331
200	114.241
250	1460.791
300	591.241
350	257.957
400	162.291

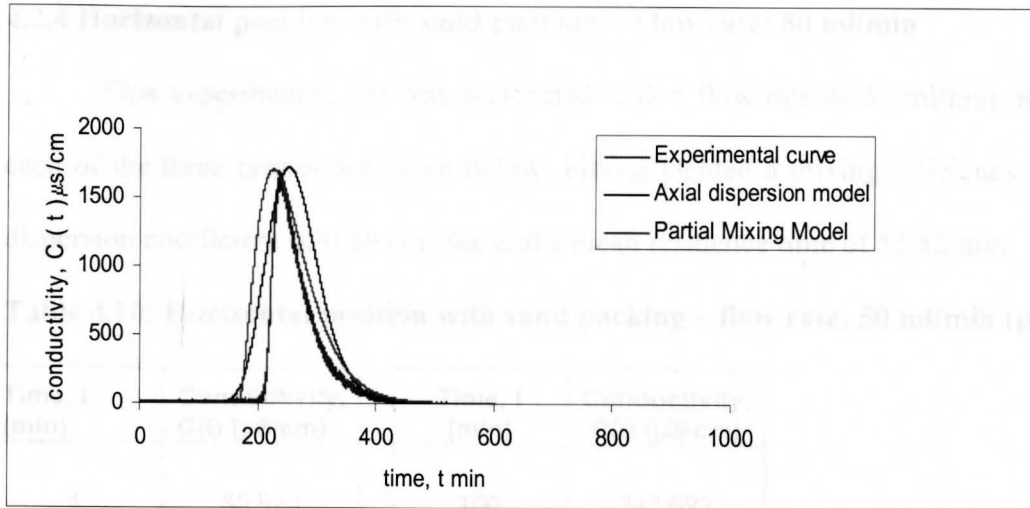


Figure 4.9: Fitting of the partial mixing model and the axial dispersion model to the experimental curve for probe 3 of the column in the inclined position with sand packing and a flow rate of 25 ml/min.

4.2.4 Horizontal position with sand packing – Flow rate: 50 ml/min

This experimental run was performed with a flow rate of 50 ml/min. Results for each of the three probes are given below. Fitting yielded a mixing efficiency of 0.43, a dispersion coefficient of $0.56 \text{ cm}^2/\text{sec}$ and a mean residence time of 55.82 min.

Table 4.10: Horizontal position with sand packing – flow rate: 50 ml/min (probe 1).

Time, t (min)	Conductivity, C(t) ($\mu\text{S}/\text{cm}$)	Time, t (min)	Conductivity, C(t) ($\mu\text{S}/\text{cm}$)
1	85.923	100	343.692
5	95.470	150	200.487
10	114.564		
20	85.923		
30	114.564		
40	3952.463		
50	4448.912		
60	2281.742		
70	1078.811		
80	658.345		
90	400.343		

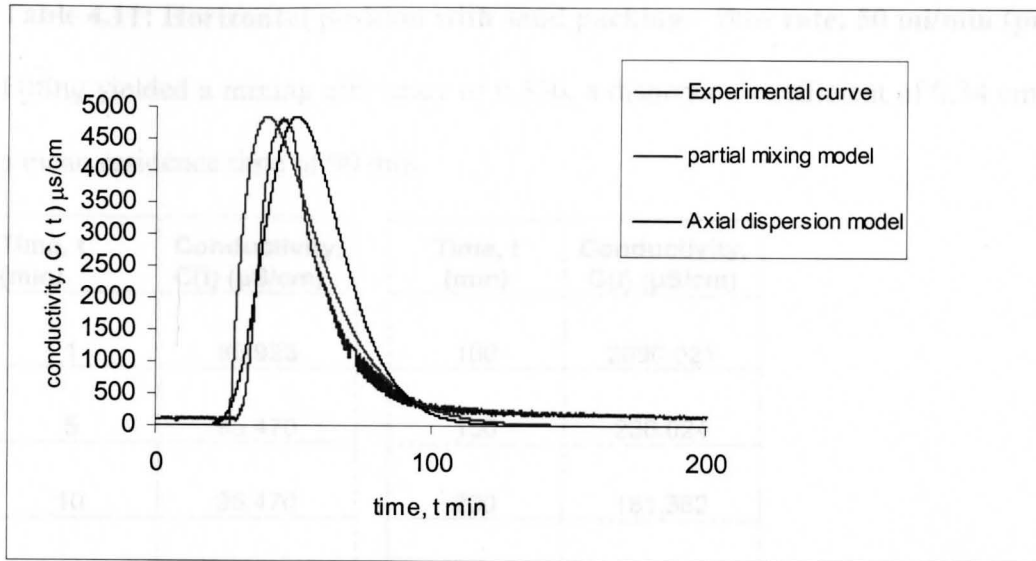


Figure 4.10: Fitting of the partial mixing model and the axial dispersion model to the experimental curve for probe 1 of the column in a horizontal position with sand packing and a flow rate of 50 ml/min.

Table 4.11: Horizontal position with sand packing – flow rate: 50 ml/min (probe 2).

Fitting yielded a mixing efficiency of 0.336, a dispersion coefficient of 0.34 cm²/sec and a mean residence time of 90 min.

Time, t (min)	Conductivity, C(t) (μS/cm)
1	85.923
5	95.470
10	95.470
20	95.470
30	105.017
40	114.564
50	114.564
60	105.017
70	391.652
80	4509.742
90	3799.841

Time, t (min)	Conductivity, C(t) (μS/cm)
100	2090.021
150	238.024
200	181.382
250	123.205
300	95.658
350	124.111
400	114.564

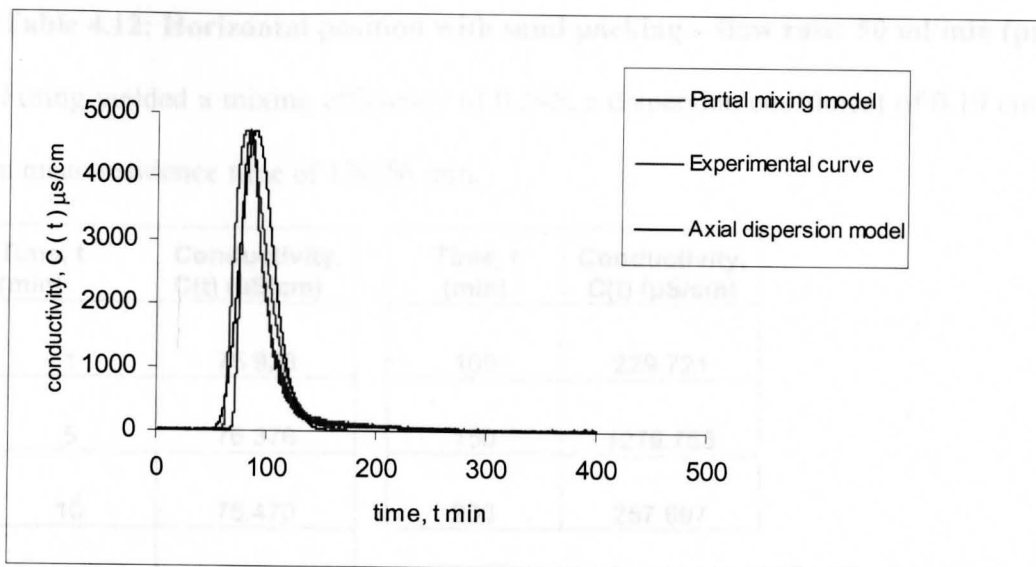


Figure 4.11: Fitting of the partial mixing model and the axial dispersion model to the experimental curve for probe 2 of the column in the horizontal position with sand packing and a flow rate of 50 ml/min.

Table 4.12: Horizontal position with sand packing – flow rate: 50 ml/min (probe 3).

Fitting yielded a mixing efficiency of 0.345, a dispersion coefficient of 0.19 cm²/sec and a mean residence time of 130.56 min.

Time, t (min)	Conductivity, C(t) (μS/cm)
1	75.923
5	76.376
10	75.470
20	85.017
30	85.017
40	95.470
50	75.470
60	95.470
70	95.470
80	95.470
90	85.923

Time, t (min)	Conductivity, C(t) (μS/cm)
100	229.721
150	1279.753
200	257.697

Figure 4.12: Fitting of the partial mixing model and the axial dispersion model to the experimental curve for probe 3 of the column in the horizontal position with sand packing and a flow rate of 50 ml/min.

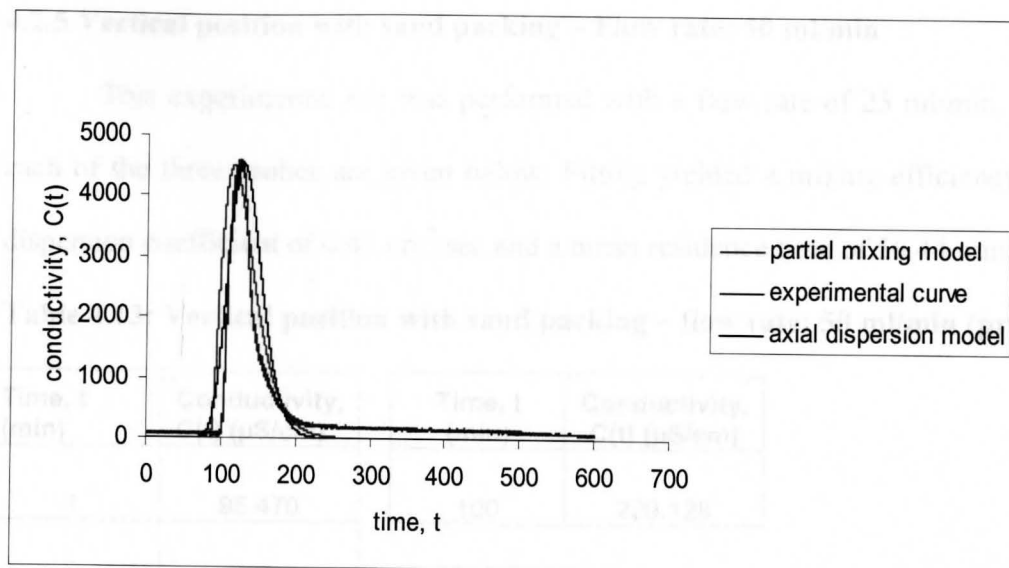


Figure 4.12: Fitting of the partial mixing model and the axial dispersion model to the experimental curve for probe 3 of the column in the horizontal position with sand packing and a flow rate of 50 ml/min.

4.2.5 Vertical position with sand packing – Flow rate: 50 ml/min

This experimental run was performed with a flow rate of 25 ml/min. Results for each of the three probes are given below. Fitting yielded a mixing efficiency of 0.47, a dispersion coefficient of $0.43 \text{ cm}^2/\text{sec}$ and a mean residence time of 56.44 min.

Table 4.13: Vertical position with sand packing – flow rate: 50 ml/min (probe 1).

Time, t (min)	Conductivity, C(t) ($\mu\text{S}/\text{cm}$)
1	95.470
5	66.829
10	76.376
20	66.829
30	353.239
40	1852.122
50	3035.951
60	2969.922
70	1728.013
80	1031.081
90	496.44

Time, t (min)	Conductivity, C(t) ($\mu\text{S}/\text{cm}$)
100	229.128

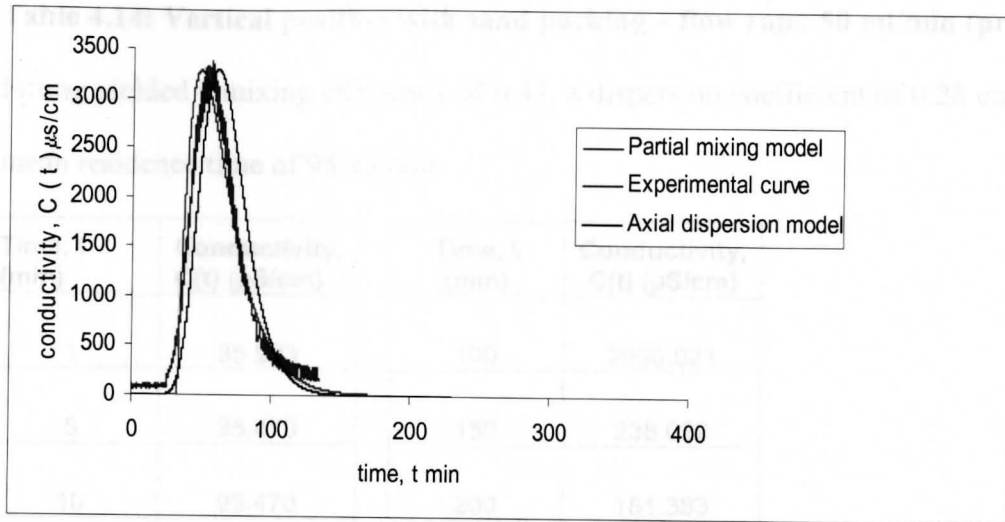


Figure 4.13: Fitting of the partial mixing model and the axial dispersion model to the experimental curve for probe 1 of the column in the vertical position with sand packing and a flow rate of 50 ml/min.

50	114.564
60	105.017
70	391.852
80	2579.741
90	3793.642

Table 4.14: Vertical position with sand packing – flow rate: 50 ml/min (probe 2).

Fitting yielded a mixing efficiency of 0.41, a dispersion coefficient of $0.28 \text{ cm}^2/\text{sec}$ and a mean residence time of 95.43 min.

Time, t (min)	Conductivity, C(t) ($\mu\text{S}/\text{cm}$)
1	85.923
5	95.470
10	95.470
20	95.470
30	105.017
40	114.564
50	114.564
60	105.017
70	391.652
80	4509.741
90	3799.842

Time, t (min)	Conductivity, C(t) ($\mu\text{S}/\text{cm}$)
100	2090.021
150	238.022
200	181.383

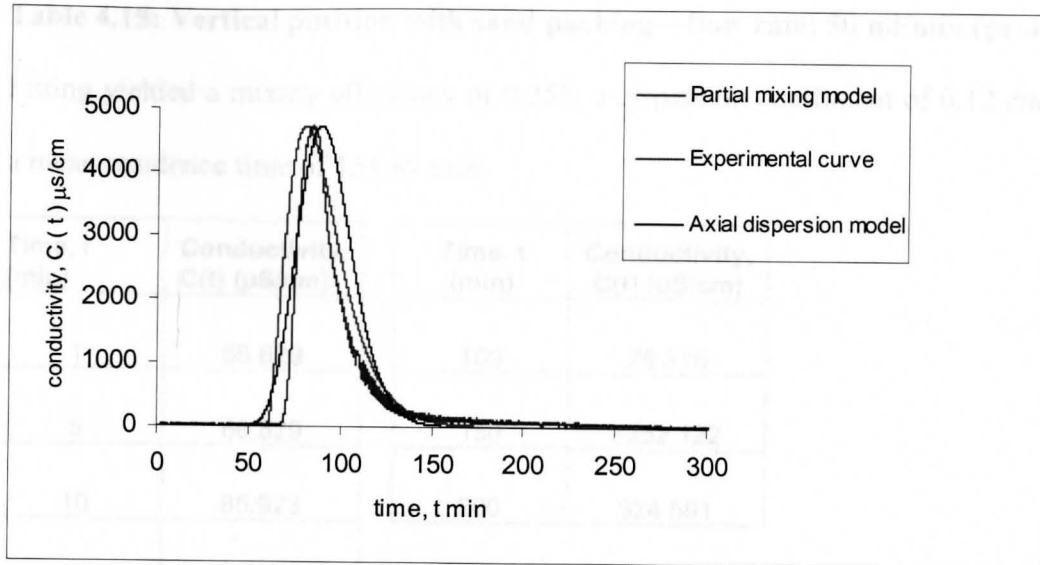


Figure 4.14: Fitting of the partial mixing model and the axial dispersion model to the experimental curve for probe 2 of the column in the vertical position with sand packing and a flow rate of 50 ml/min.

Table 4.15: Vertical position with sand packing – flow rate: 50 ml/min (probe 3).

Fitting yielded a mixing efficiency of 0.255, a dispersion coefficient of $0.12 \text{ cm}^2/\text{sec}$ and a mean residence time of 151.89 min.

Time, t (min)	Conductivity, C(t) ($\mu\text{S}/\text{cm}$)
1	66.829
5	66.829
10	85.923
20	95.470
30	85.923
40	57.282
50	76.376
60	57.282
70	76.376
80	76.376
90	66.829

Time, t (min)	Conductivity, C(t) ($\mu\text{S}/\text{cm}$)
100	76.376
150	3252.122
200	324.591

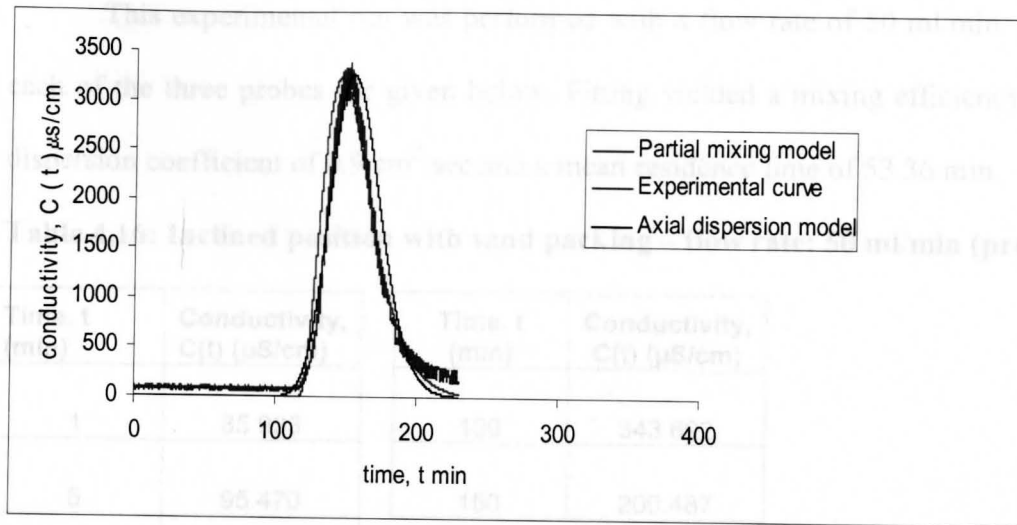


Figure 4.15: Fitting of the partial mixing model and the axial dispersion model to the experimental curve for probe 3 of the column in the vertical position with sand packing and a flow rate of 50 ml/min.

4.2.6 Inclined position with sand packing – Flow rate: 50 ml/min

This experimental run was performed with a flow rate of 50 ml/min. Results for each of the three probes are given below. Fitting yielded a mixing efficiency of 0.48, a dispersion coefficient of $0.9 \text{ cm}^2/\text{sec}$ and a mean residence time of 53.36 min.

Table 4.16: Inclined position with sand packing – flow rate: 50 ml/min (probe 1).

Time, t (min)	Conductivity, C(t) ($\mu\text{S}/\text{cm}$)	Time, t (min)	Conductivity, C(t) ($\mu\text{S}/\text{cm}$)
1	85.923	100	343.692
5	95.470	150	200.487
10	114.564		
20	85.923		
30	114.564		
40	3952.461		
50	4448.912		
60	2281.743		
70	1078.814		
80	658.347		
90	400.341		

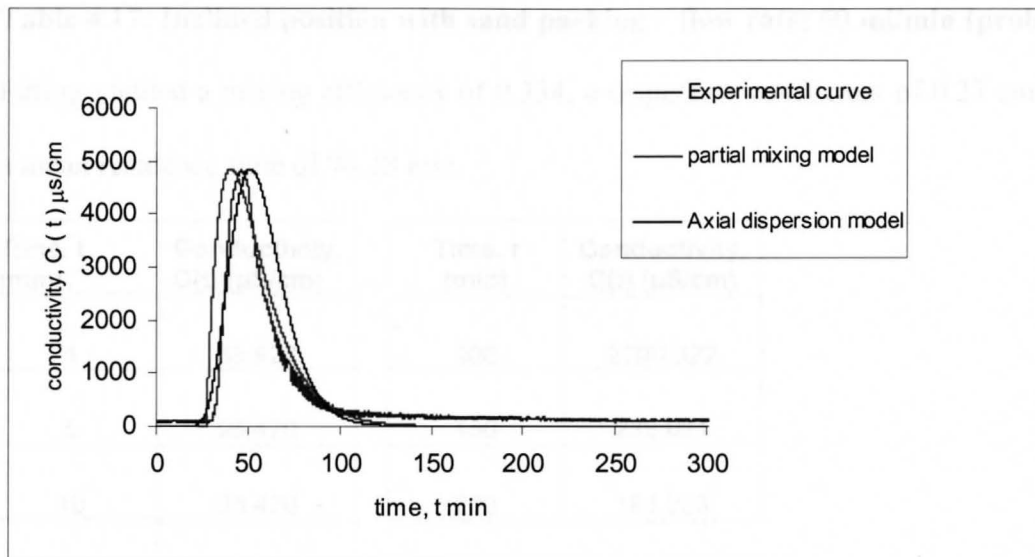


Figure 4.16: Fitting of the partial mixing model and the axial dispersion model to the experimental curve for probe 1 of the column in the inclined position with sand packing and a flow rate of 50 ml/min.

Table 4.17: Inclined position with sand packing – flow rate: 50 ml/min (probe 2).

Fitting yielded a mixing efficiency of 0.334, a dispersion coefficient of $0.27 \text{ cm}^2/\text{sec}$ and a mean residence time of 90.28 min.

Time, t (min)	Conductivity, C(t) ($\mu\text{S}/\text{cm}$)
1	85.923
5	95.470
10	95.470
20	95.470
30	105.017
40	114.564
50	114.564
60	105.017
70	391.653
80	4509.742
90	3799.841

Time, t (min)	Conductivity, C(t) ($\mu\text{S}/\text{cm}$)
100	2090.022
150	238.021
200	181.383

Figure 4.17: Fitting of the partial mixing model and the axial dispersion model to the experimental curve for probe 2 of the column in the inclined position with sand packing and a flow rate of 50 ml/min.

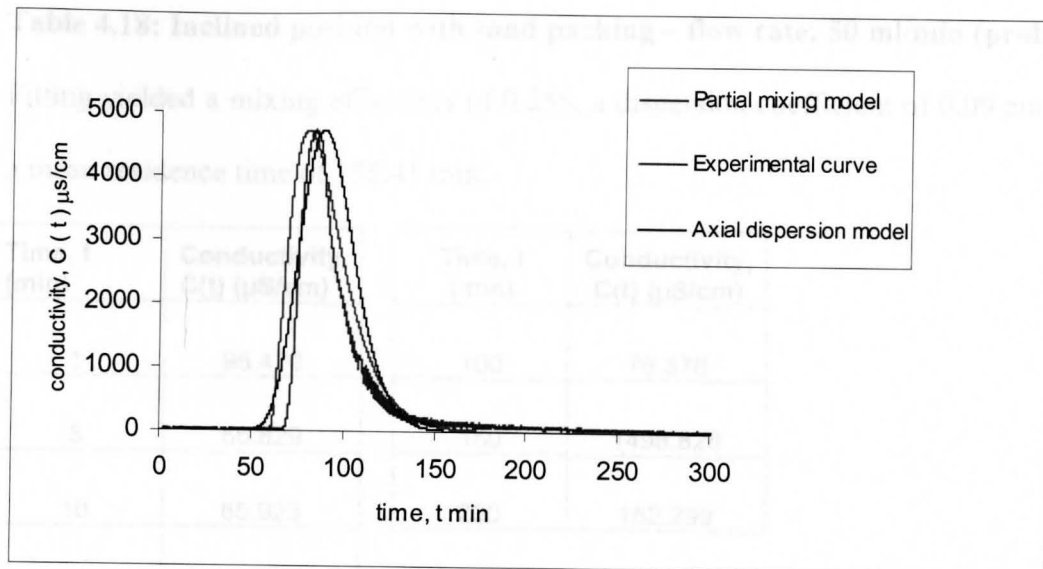


Figure 4.17: Fitting of the partial mixing model and the axial dispersion model to the experimental curve for probe 2 of the column in the inclined position with sand packing and a flow rate of 50 ml/min.

Table 4.18: Inclined position with sand packing – flow rate: 50 ml/min (probe 3).

Fitting yielded a mixing efficiency of 0.255, a dispersion coefficient of $0.09 \text{ cm}^2/\text{sec}$ and a mean residence time of 155.41 min.

Time, t (min)	Conductivity, C(t) ($\mu\text{S}/\text{cm}$)
1	95.470
5	66.829
10	85.923
20	76.376
30	57.282
40	66.829
50	76.376
60	76.376
70	66.829
80	85.923
90	66.829

Time, t (min)	Conductivity, C(t) ($\mu\text{S}/\text{cm}$)
100	76.376
150	1498.828
200	162.299

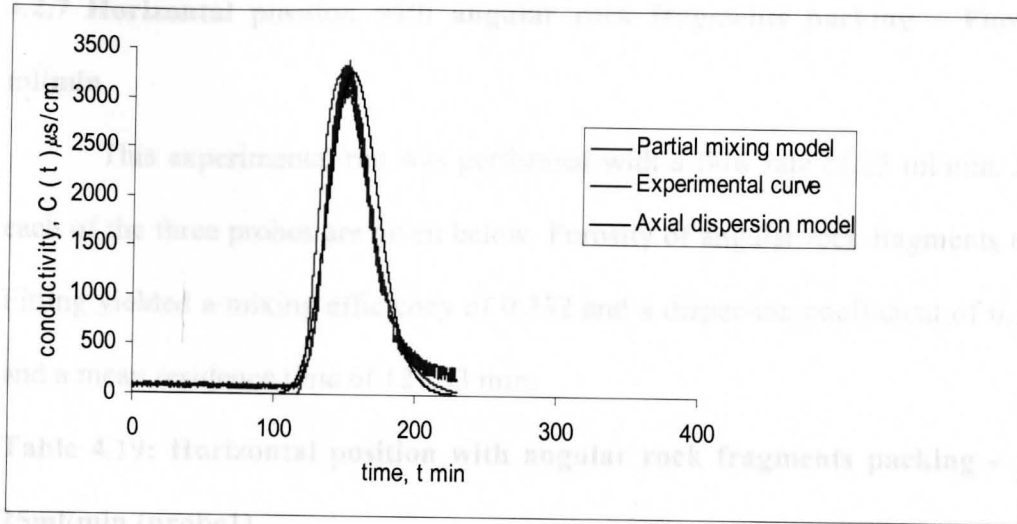


Figure 4.18: Fitting of the partial mixing model and the axial dispersion model to the experimental curve for probe 3 of the column in the inclined position with sand packing and a flow rate of 50 ml/min.

Time, t (min)	Conductivity, C(t) (µs/cm)	Time, t (min)	Conductivity, C(t) (µs/cm)
1	75.376	160	1270.751
5	75.470	200	257.897
10	85.017		
30	85.017		
40	85.470		
50	75.470		
60	85.470		
70	85.470		
80	90.470		
90	85.823		

4.2.7 Horizontal position with angular rock fragments packing – Flow rate: 25 ml/min

This experimental run was performed with a flow rate of 25 ml/min. Results for each of the three probes are given below. Porosity of angular rock fragments used is 0.5. Fitting yielded a mixing efficiency of 0.332 and a dispersion coefficient of $0.17 \text{ cm}^2/\text{sec}$ and a mean residence time of 127.53 min.

Table 4.19: Horizontal position with angular rock fragments packing – flow rate: 25ml/min (probe1).

Time, t (min)	Conductivity, C(t) ($\mu\text{S}/\text{cm}$)
1	75.923
5	76.376
10	75.470
20	85.017
30	85.017
40	95.470
50	75.470
60	95.470
70	95.470
80	95.470
90	85.923

Time, t (min)	Conductivity, C(t) ($\mu\text{S}/\text{cm}$)
100	229.722
150	1279.751
200	257.697

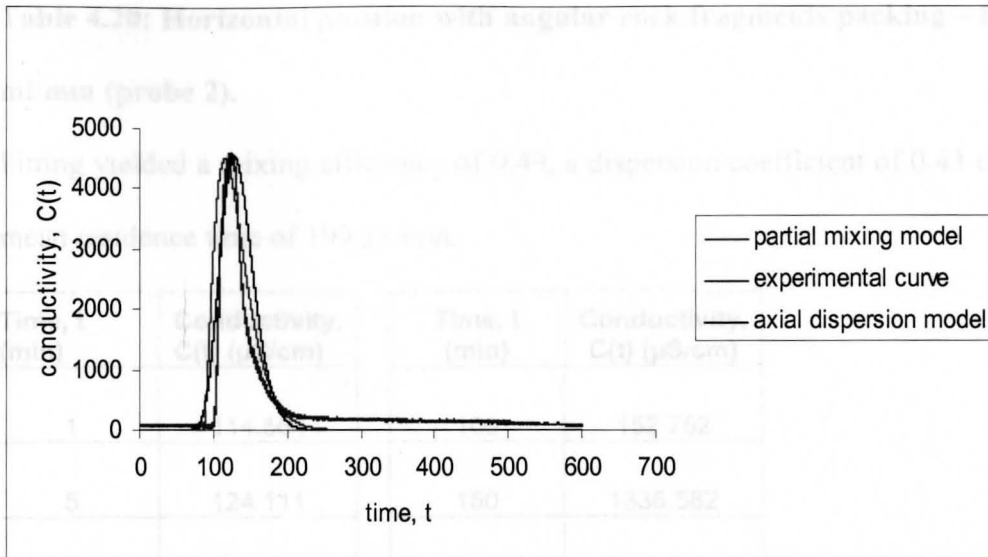


Figure 4.19: Fitting of the partial mixing model and the axial dispersion model to the experimental curve for probe 1 of the column in the horizontal position with angular rock fragments packing and a flow rate of 25 ml/min.

Table 4.20: Horizontal position with angular rock fragments packing – flow rate: 25 ml/min (probe 2).

Fitting yielded a mixing efficiency of 0.49, a dispersion coefficient of $0.43 \text{ cm}^2/\text{sec}$ and a mean residence time of 199.35 min.

Time, t (min)	Conductivity, C(t) ($\mu\text{S}/\text{cm}$)
1	114.564
5	124.111
10	105.017
20	124.111
30	95.470
40	114.564
50	105.017
60	105.017
70	114.564
80	124.111
90	114.564

Time, t (min)	Conductivity, C(t) ($\mu\text{S}/\text{cm}$)
100	152.752
150	1336.582
200	1374.771
250	1346.132
300	458.256
350	400.974
400	286.415

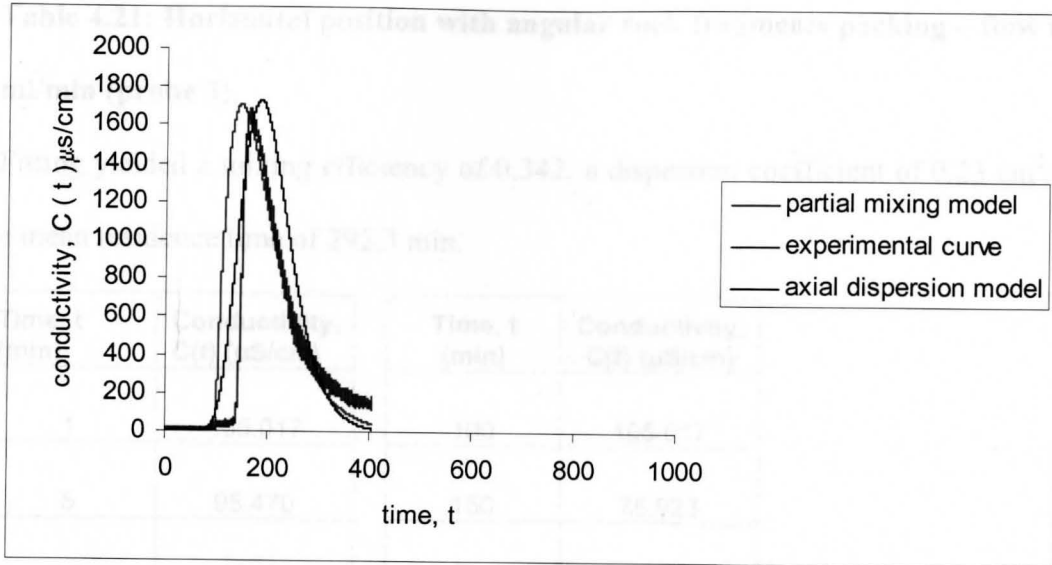


Figure 4.20: Fitting of the partial mixing model and the axial dispersion model to the experimental curve for probe 2 of the column in the horizontal position with angular rock fragments packing and a flow rate of 25 ml/min.

Table 4.21: Horizontal position with angular rock fragments packing – flow rate: 25 ml/min (probe 3).

Fitting yielded a mixing efficiency of 0.342, a dispersion coefficient of 0.23 cm²/sec and a mean residence time of 292.3 min.

Time, t (min)	Conductivity, C(t) (μS/cm)
1	105.017
5	95.470
10	114.564
20	105.017
30	105.017
40	105.017
50	85.923
60	95.470
70	94.564
80	85.923
90	114.564

Time, t (min)	Conductivity, C(t) (μS/cm)
100	105.017
150	75.923
200	112.923
250	1117.021
300	792.853
350	420.325
400	286.417
500	181.589

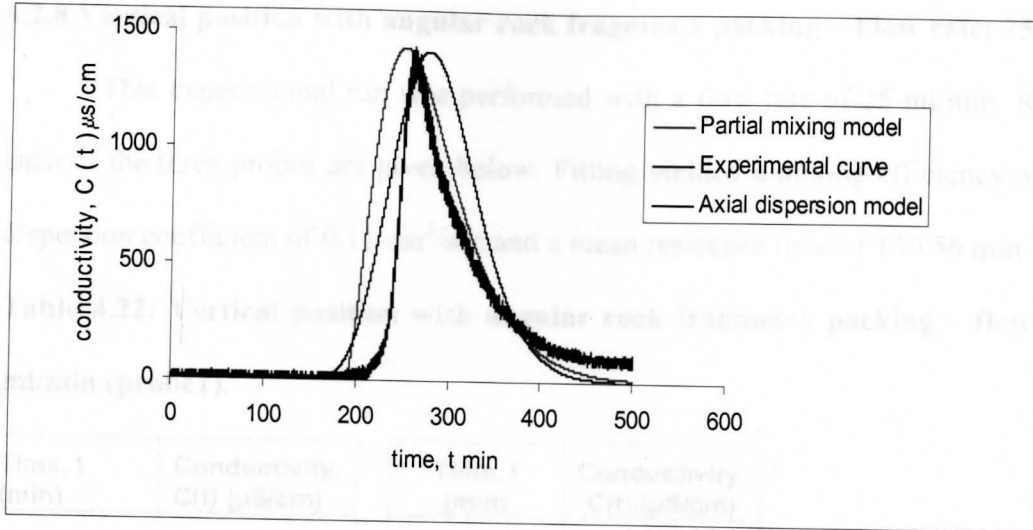


Figure 4.21: Fitting of the partial mixing model and the axial dispersion model to the experimental curve for probe 3 of the column in the horizontal position with angular rock fragments packing and a flow rate of 25 ml/min.

4.2.8 Vertical position with angular rock fragments packing – Flow rate: 25 ml/min

This experimental run was performed with a flow rate of 25 ml/min. Results for each of the three probes are given below. Fitting yielded a mixing efficiency of 0.285, a dispersion coefficient of $0.11 \text{ cm}^2/\text{sec}$ and a mean residence time of 130.56 min.

Table 4.22: Vertical position with angular rock fragments packing – flow rate: 25 ml/min (probe1).

Time, t (min)	Conductivity, C(t) ($\mu\text{S}/\text{cm}$)
1	95.470
5	66.829
10	76.376
20	66.829
30	85.923
40	66.829
50	66.829
60	85.923
70	66.829
80	76.373
90	133.658

Time, t (min)	Conductivity, C(t) ($\mu\text{S}/\text{cm}$)
100	381.881
150	1002.442
200	229.128

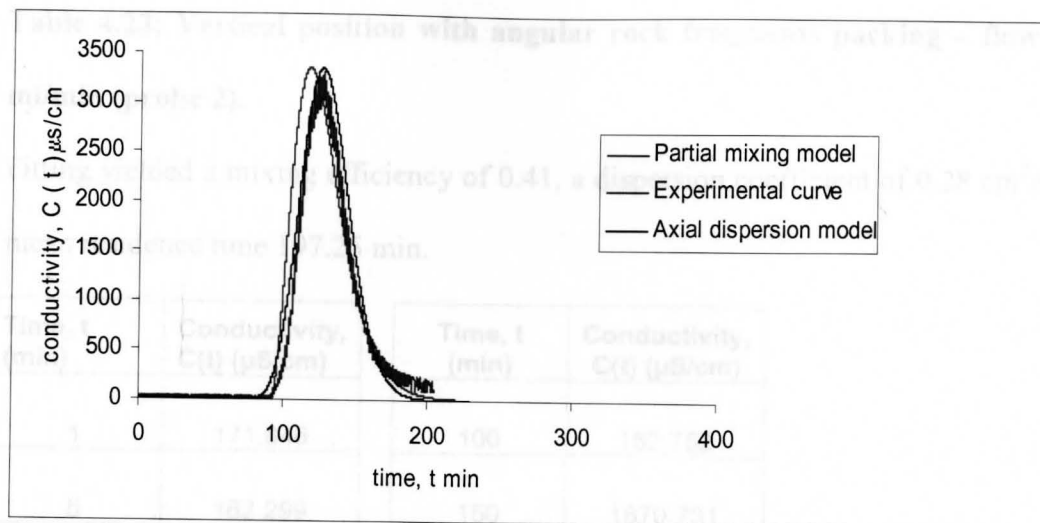


Figure 4.22: Fitting of the partial mixing model and the axial dispersion model to the experimental curve for probe 1 of the column in the vertical position with angular rock fragments packing and a flow rate of 25 ml/min.

Table 4.23: Vertical position with angular rock fragments packing – flow rate: 25 ml/min (probe 2).

Fitting yielded a mixing efficiency of 0.41, a dispersion coefficient of 0.28 cm²/sec and a mean residence time 197.25 min.

Time, t (min)	Conductivity, C(t) (μS/cm)
1	171.846
5	162.299
10	152.752
20	152.752
30	133.658
40	143.205
50	143.205
60	133.658
70	162.299
80	181.393
90	152.752

Time, t (min)	Conductivity, C(t) (μS/cm)
100	152.752
150	1670.731
200	1622.991
250	1699.372
300	205.504
350	165.957

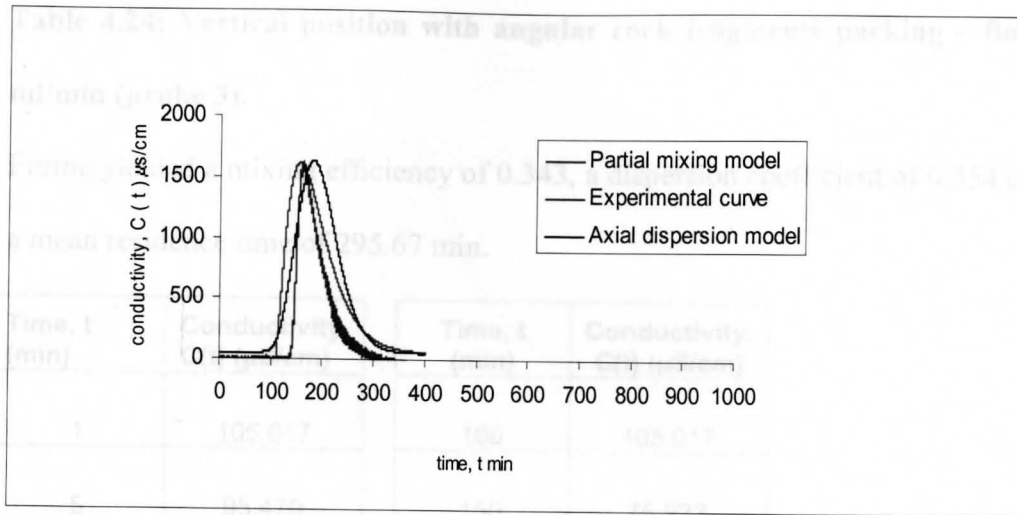


Figure 4.23: Fitting of the partial mixing model and the axial dispersion model to the experimental curve for probe 2 of the column in the vertical position with angular rock fragments packing and a flow rate of 25 ml/min.

Table 4.24: Vertical position with angular rock fragments packing – flow rate: 25 ml/min (probe 3).

Fitting yielded a mixing efficiency of 0.343, a dispersion coefficient of $0.354 \text{ cm}^2/\text{sec}$ and a mean residence time of 295.67 min.

Time, t (min)	Conductivity, C(t) ($\mu\text{S}/\text{cm}$)
1	105.017
5	95.470
10	114.564
20	105.017
30	105.017
40	105.017
50	85.923
60	95.470
70	94.564
80	85.923
90	114.564

Time, t (min)	Conductivity, C(t) ($\mu\text{S}/\text{cm}$)
100	105.017
150	75.923
200	112.922
250	1117.021
300	792.851
350	420.325
400	286.413
500	181.582

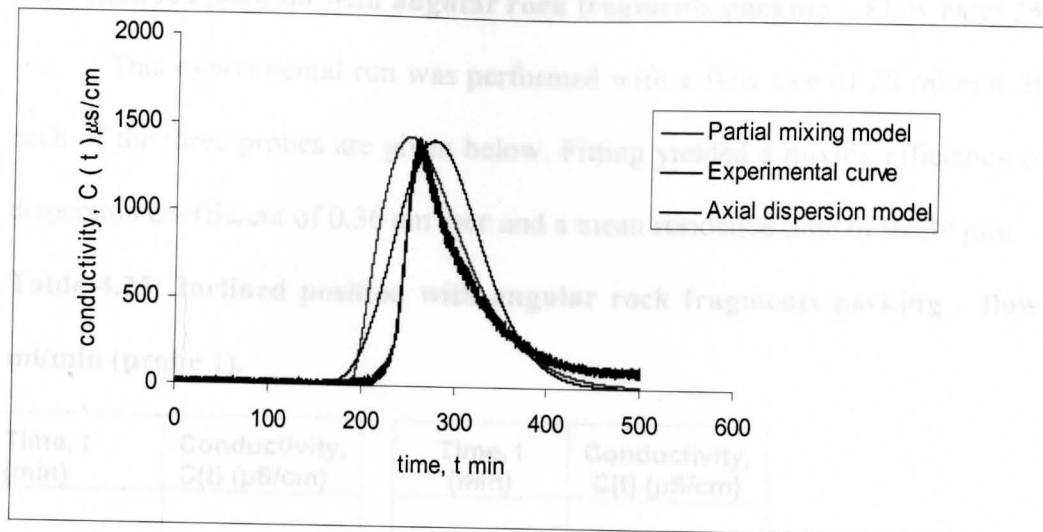


Figure 4.24: Fitting of the partial mixing model and the axial dispersion model to the experimental curve for probe 3 of the column in the vertical position with angular rock fragments packing and a flow rate of 25 ml/min.

4.2.9 Inclined position with angular rock fragments packing – Flow rate: 25 ml/min

This experimental run was performed with a flow rate of 25 ml/min. Results for each of the three probes are given below. Fitting yielded a mixing efficiency of 0.421, a dispersion coefficient of $0.36 \text{ cm}^2/\text{sec}$ and a mean residence time of 97.39 min.

Table 4.25: Inclined position with angular rock fragments packing – flow rate: 25 ml/min (probe 1).

Time, t (min)	Conductivity, C(t) ($\mu\text{S}/\text{cm}$)
1	95.470
5	95.470
10	95.470
20	95.470
30	95.470
40	105.017
50	248.222
60	238.675
70	229.128
80	3856.992
90	3799.711

Time, t (min)	Conductivity, C(t) ($\mu\text{S}/\text{cm}$)
100	1050.173
150	143.202

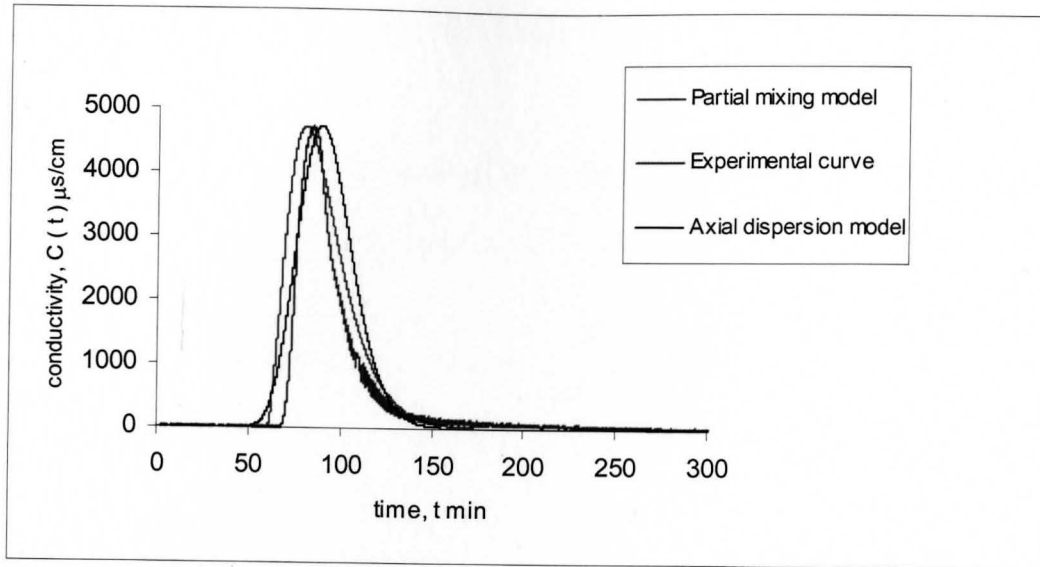


Figure 4.25: Fitting of the partial mixing model and the axial dispersion model to the experimental curve for probe 1 of the column in the inclined position with angular rock fragments packing and a flow rate of 25 ml/min.

Table 4.26: Inclined position with angular rock fragments packing – flow rate: 25 ml/min (probe 2).

Fitting yielded a mixing efficiency of 0.412 and a dispersion coefficient of 0.283 cm²/sec and a mean residence time of 190.88 min.

Time, t (min)	Conductivity, C(t) (μS/cm)
1	171.846
5	162.299
10	152.752
20	152.752
30	133.658
40	143.205
50	143.205
60	133.658
70	162.299
80	181.393
90	152.752

Time, t (min)	Conductivity, C(t) (μS/cm)
100	152.752
150	1670.732
200	1622.991
250	1699.372
300	205.504
350	165.957

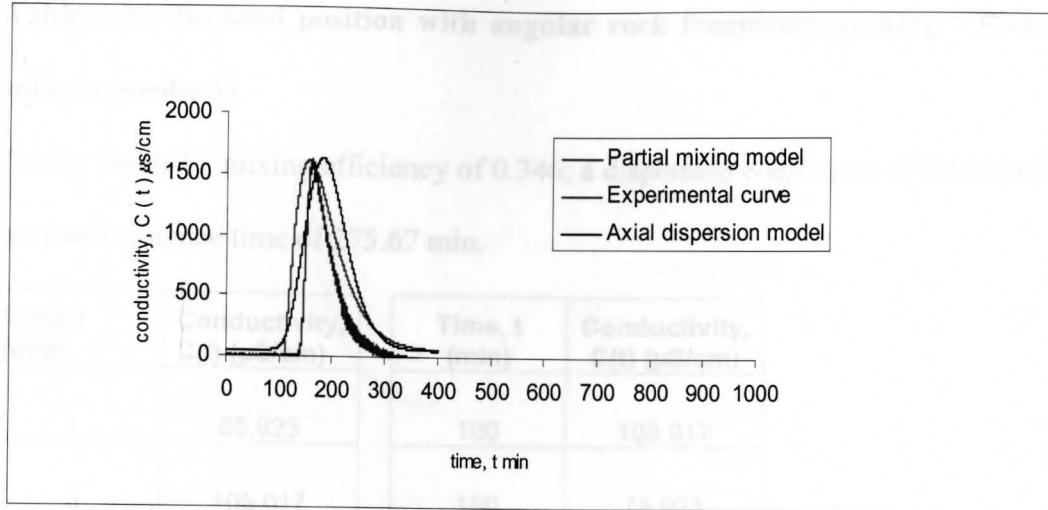


Figure 4.26: Fitting of the partial mixing model and the axial dispersion model to the experimental curve for probe 2 of the column in the inclined position with angular rock fragments packing and a flow rate of 25 ml/min.

Table 4.27: Inclined position with angular rock fragments packing – flow rate: 25 ml/min (probe 3).

Fitting yielded a mixing efficiency of 0.346, a dispersion coefficient of 0.189 cm²/sec and a mean residence time of 275.67 min.

Time, t (min)	Conductivity, C(t) (µS/cm)	Time, t (min)	Conductivity, C(t) (µS/cm)
1	85.923	100	105.017
5	105.017	150	75.923
10	105.017	200	114.223
20	95.470	250	1116.151
30	95.470	300	792.523
40	105.017	350	459.612
50	85.923	400	286.068
60	95.470	450	181.068
70	95.470	500	181.393
80	114.564		
90	114.564		

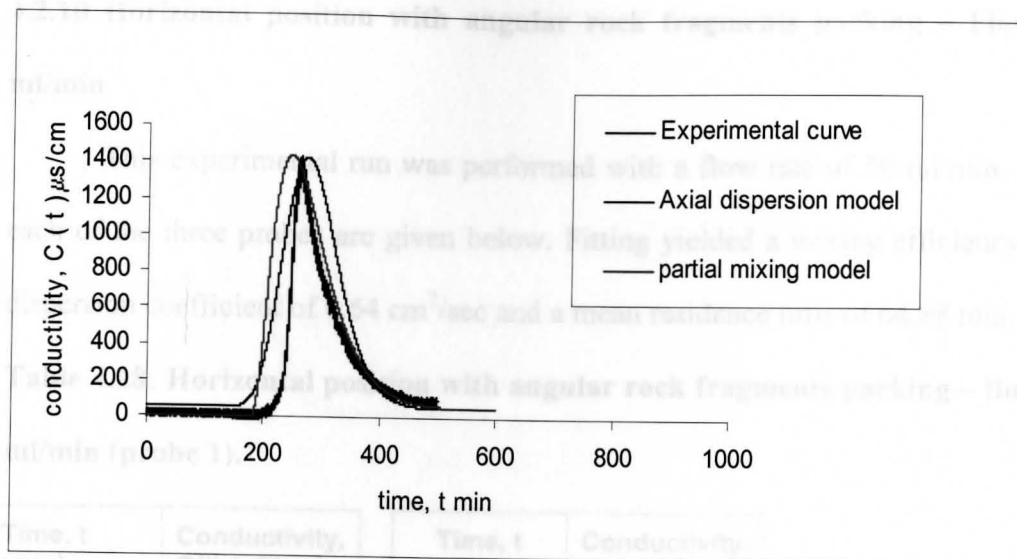


Figure 4.27: Fitting of the partial mixing model and the axial dispersion model to the experimental curve for probe 3 of the column in the inclined position with angular rock fragments packing and a flow rate of 25 ml/min.

4.2.10 Horizontal position with angular rock fragments packing – Flow rate: 50 ml/min

This experimental run was performed with a flow rate of 50 ml/min. Results for each of the three probes are given below. Fitting yielded a mixing efficiency of 0.43, a dispersion coefficient of $0.64 \text{ cm}^2/\text{sec}$ and a mean residence time of 64.88 min.

Table 4.28: Horizontal position with angular rock fragments packing – flow rate: 50 ml/min (probe 1).

Time, t (min)	Conductivity, C(t) ($\mu\text{S}/\text{cm}$)
1	85.923
5	95.470
10	114.564
20	85.923
30	114.564
40	3952.462
50	4448.911
60	2281.744
70	1078.817
80	658.344
90	400.346

Time, t (min)	Conductivity, C(t) ($\mu\text{S}/\text{cm}$)
100	343.692
150	200.487

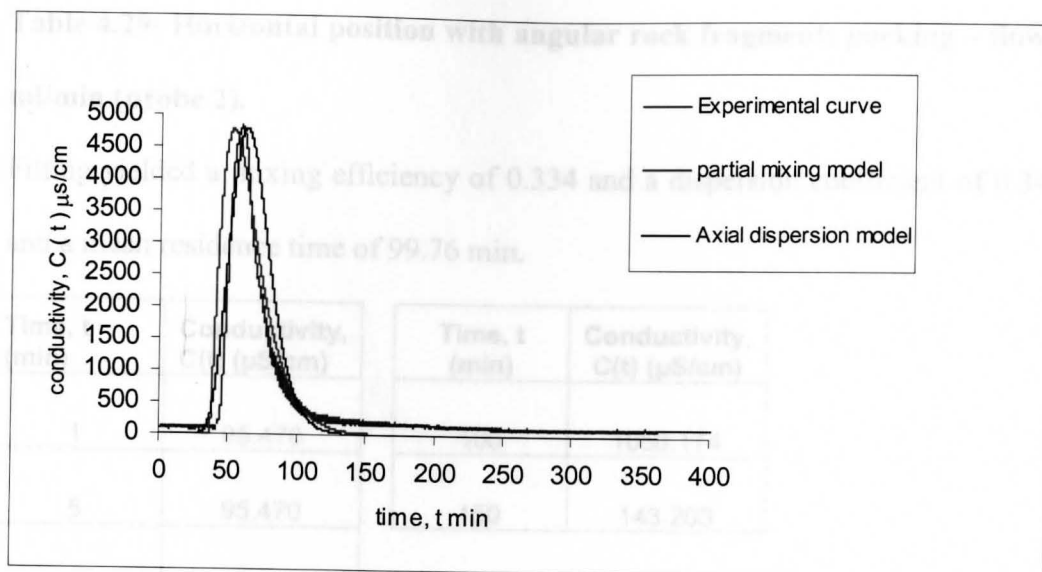


Figure 4.28: Fitting of the partial mixing model and the axial dispersion model to the experimental curve for probe 1 of the column in the horizontal position with angular rock fragments packing and a flow rate of 50 ml/min.

Table 4.29: Horizontal position with angular rock fragments packing – flow rate: 50 ml/min (probe 2).

Fitting yielded a mixing efficiency of 0.334 and a dispersion coefficient of 0.34 cm²/sec and a mean residence time of 99.76 min.

Time, t (min)	Conductivity, C(t) (µS/cm)
1	95.470
5	95.470
10	95.470
20	95.470
30	95.470
40	105.017
50	248.222
60	238.675
70	229.128
80	3856.992
90	3799.711

Time, t (min)	Conductivity, C(t) (µS/cm)
100	1050.174
150	143.203

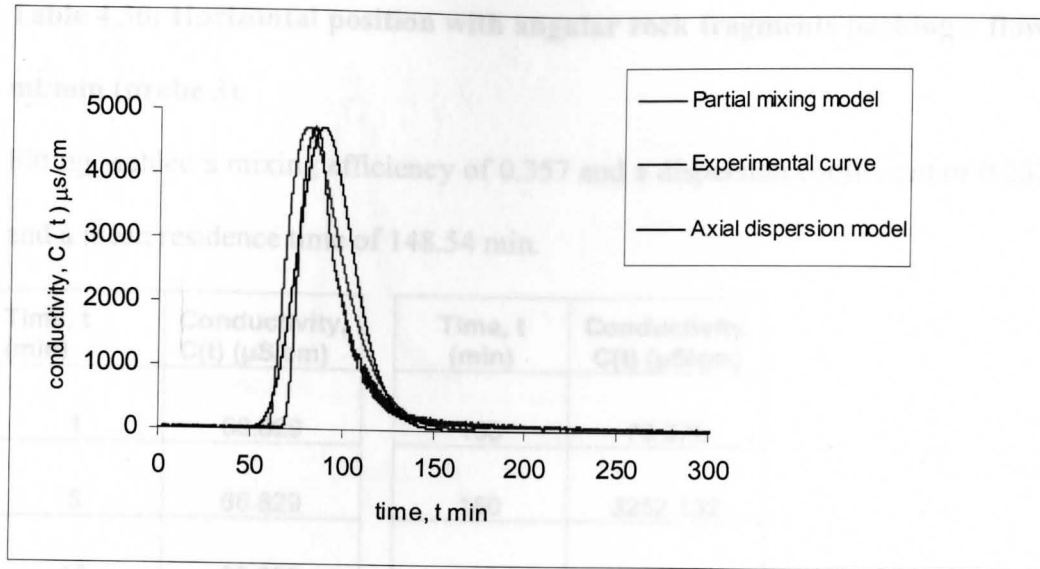


Figure 4.29: Fitting of the partial mixing model and the axial dispersion model to the experimental curve for probe 2 of the column in the horizontal position with angular rock fragments packing and a flow rate of 50 ml/min.

Table 4.30: Horizontal position with angular rock fragments packing – flow rate: 50 ml/min (probe 3).

Fitting yielded a mixing efficiency of 0.357 and a dispersion coefficient of 0.232 cm²/sec and a mean residence time of 148.54 min.

Time, t (min)	Conductivity, C(t) (μS/cm)
1	66.829
5	66.829
10	85.923
20	95.470
30	85.923
40	57.282
50	76.376
60	57.282
70	76.376
80	76.376
90	66.829

Time, t (min)	Conductivity, C(t) (μS/cm)
100	76.376
150	3252.132
200	324.591

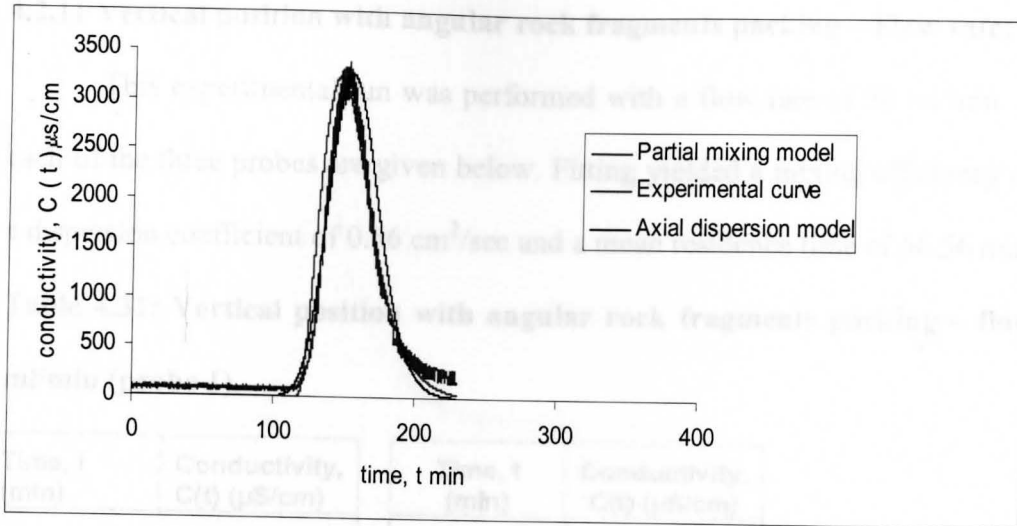


Figure 4.30: Fitting of the partial mixing model and the axial dispersion model to the experimental curve for probe 3 of the column in the horizontal position with angular rock fragments packing and a flow rate of 50 ml/min.

4.2.11 Vertical position with angular rock fragments packing – Flow rate: 50 ml/min

This experimental run was performed with a flow rate of 50 ml/min. Results for each of the three probes are given below. Fitting yielded a mixing efficiency of 0.41 and a dispersion coefficient of $0.56 \text{ cm}^2/\text{sec}$ and a mean residence time of 66.56 min.

Table 4.31: Vertical position with angular rock fragments packing – flow rate: 50 ml/min (probe 1).

Time, t (min)	Conductivity, C(t) ($\mu\text{S}/\text{cm}$)	Time, t (min)	Conductivity, C(t) ($\mu\text{S}/\text{cm}$)
1	95.470	100	654.177
5	95.470	150	143.204
10	95.470		
20	95.470		
30	95.470		
40	105.013		
50	248.222		
60	4856.675		
70	3678.128		
80	2656.993		
90	1099.711		

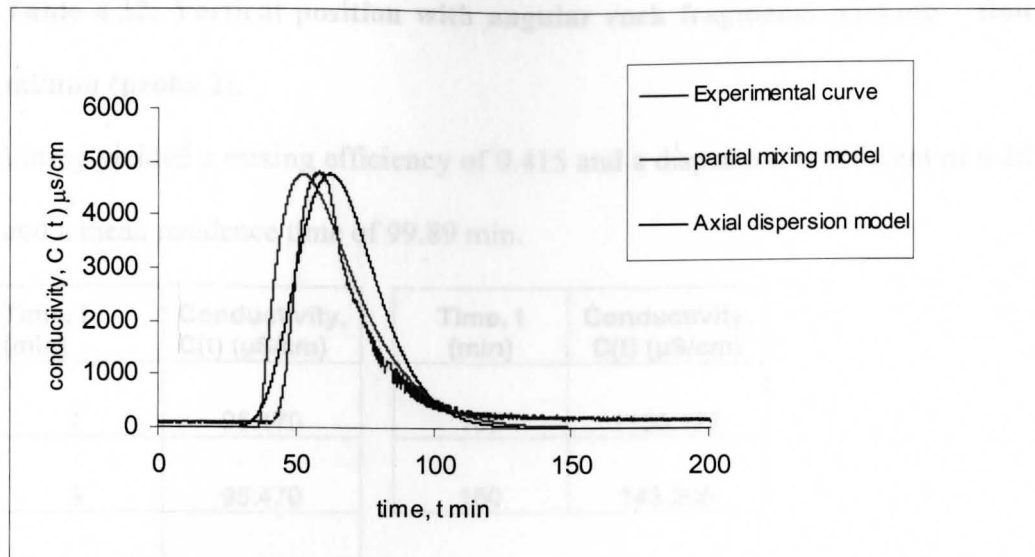


Figure 4.31: Fitting of the partial mixing model and the axial dispersion model to the experimental curve for probe 1 of the column in the vertical position with angular rock fragments packing and a flow rate of 50 ml/min.

Table 4.32: Vertical position with angular rock fragments packing – flow rate: 50 ml/min (probe 2).

Fitting yielded a mixing efficiency of 0.415 and a dispersion coefficient of 0.282 cm²/sec and a mean residence time of 99.89 min.

Time, t (min)	Conductivity, C(t) (μS/cm)
1	95.470
5	95.470
10	95.470
20	95.470
30	95.470
40	105.017
50	248.222
60	238.675
70	229.128
80	3856.993
90	3799.711

Time, t (min)	Conductivity, C(t) (μS/cm)
100	1150.177
150	143.205

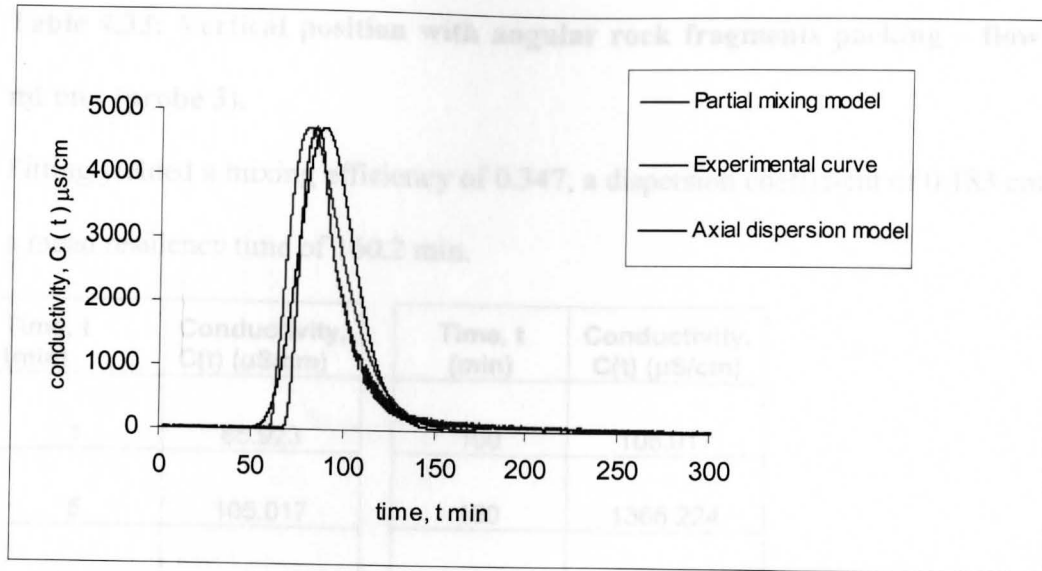


Figure 4.32: Fitting of the partial mixing model and the axial dispersion model to the experimental curve for probe 2 of the column in the vertical position with angular rock fragments packing and a flow rate of 50 ml/min.

Table 4.33: Vertical position with angular rock fragments packing – flow rate: 50 ml/min (probe 3).

Fitting yielded a mixing efficiency of 0.347, a dispersion coefficient of 0.183 cm²/sec and a mean residence time of 160.2 min.

Time, t (min)	Conductivity, C(t) (µS/cm)	Time, t (min)	Conductivity, C(t) (µS/cm)
1	85.923	100	105.017
5	105.017	150	1365.224
10	105.017	200	951.151
20	95.470	250	142.546
30	95.470		
40	105.017		
50	85.923		
60	95.470		
70	95.470		
80	114.564		
90	114.564		

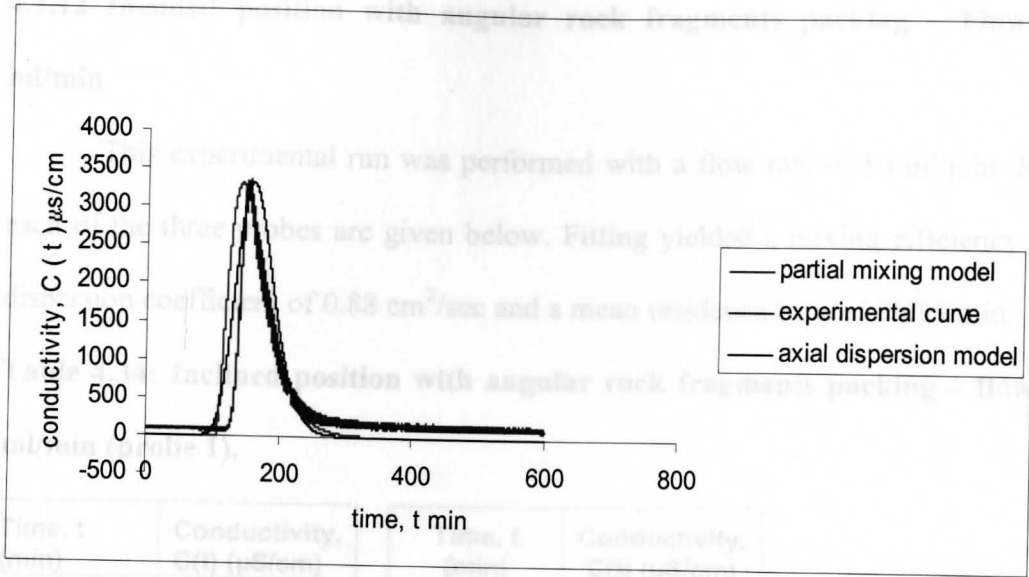


Figure 4.33: Fitting of the partial mixing model and the axial dispersion model to the experimental curve for probe 3 of the column in the vertical position with angular rock fragments packing and a flow rate of 50 ml/min.

4.2.12 Inclined position with angular rock fragments packing – Flow rate: 50 ml/min

This experimental run was performed with a flow rate of 50 ml/min. Results for each of the three probes are given below. Fitting yielded a mixing efficiency of 0.44, a dispersion coefficient of $0.88 \text{ cm}^2/\text{sec}$ and a mean residence time of 59.89 min.

Table 4.34: Inclined position with angular rock fragments packing – flow rate: 50 ml/min (probe 1).

Time, t (min)	Conductivity, C(t) ($\mu\text{S}/\text{cm}$)	Time, t (min)	Conductivity, C(t) ($\mu\text{S}/\text{cm}$)
1	95.470	100	305.047
5	95.470		
10	95.470		
20	114.564		
30	257.769		
40	2579.094		
50	4172.041		
60	4286.613		
70	3055.048		
80	1145.645		
90	400.974		

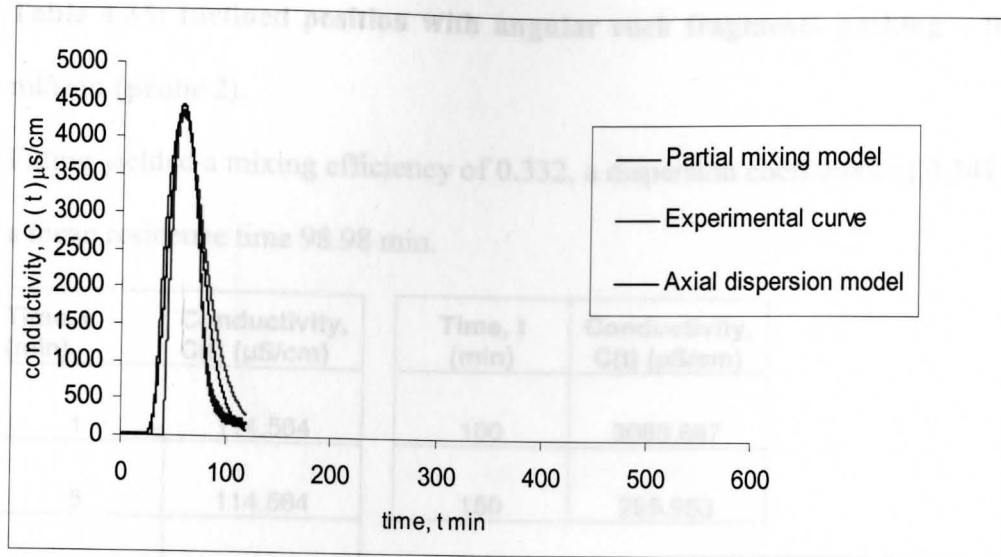


Figure 4.34: Fitting of the partial mixing model and the axial dispersion model to the experimental curve for probe 1 of the column in the inclined position with angular rock fragments packing and a flow rate of 50 ml/min.

Table 4.35: Inclined position with angular rock fragments packing – flow rate: 50 ml/min (probe 2).

Fitting yielded a mixing efficiency of 0.332, a dispersion coefficient of 0.341 cm²/sec and a mean residence time 98.98 min.

Time, t (min)	Conductivity, C(t) (μS/cm)
1	114.564
5	114.564
10	95.470
20	114.564
30	105.017
40	95.470
50	257.769
60	1966.683
70	2014.421
80	2014.424
90	2052.613

Time, t (min)	Conductivity, C(t) (μS/cm)
100	3083.687
150	295.953

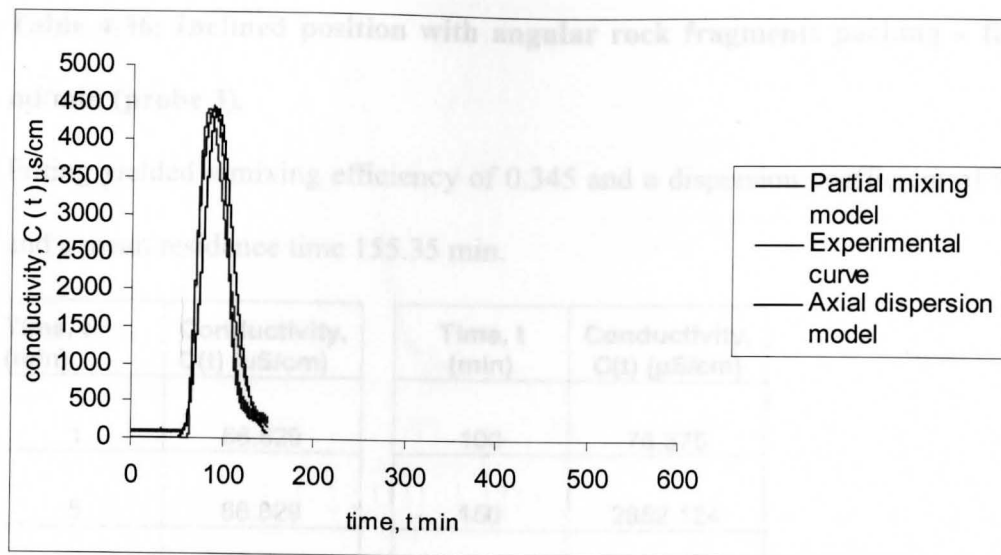


Figure 4.35: Fitting of the partial mixing model and the axial dispersion model to the experimental curve for probe 2 of the column in the inclined position with angular rock fragments packing and a flow rate of 50 ml/min.

Table 4.36: Inclined position with angular rock fragments packing – flow rate: 50 ml/min (probe 3).

Fitting yielded a mixing efficiency of 0.345 and a dispersion coefficient of $0.36 \text{ cm}^2/\text{sec}$ and a mean residence time 155.35 min.

Time, t (min)	Conductivity, C(t) ($\mu\text{S}/\text{cm}$)
1	66.829
5	66.829
10	85.923
20	95.470
30	85.923
40	57.282
50	76.376
60	57.282
70	76.376
80	76.376
90	66.829

Time, t (min)	Conductivity, C(t) ($\mu\text{S}/\text{cm}$)
100	76.376
150	2852.124
200	162.299

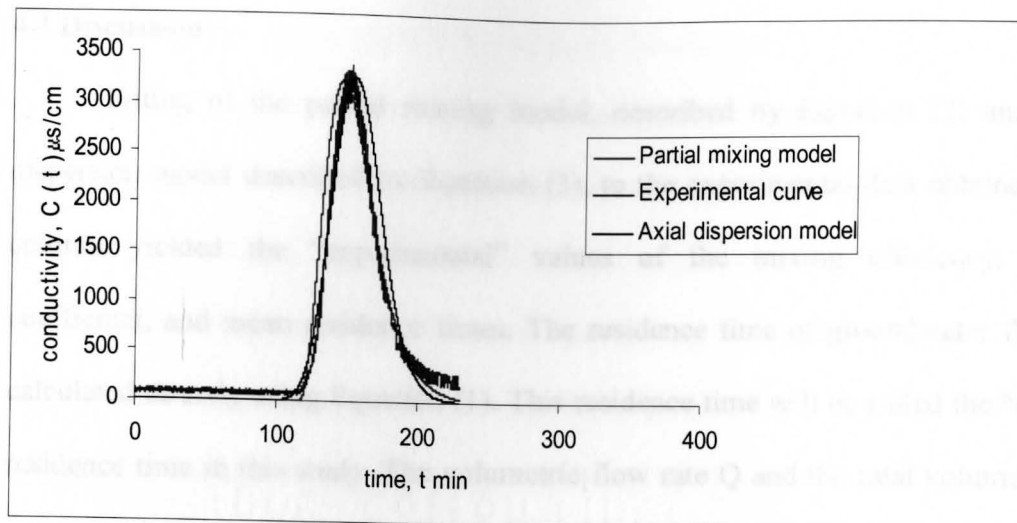


Figure 4.36: Fitting of the partial mixing model and the axial dispersion model to the experimental curve for probe 3 of the column in the inclined position with angular rock fragments packing and a flow rate of 50 ml/min.

The experimental residence time values did not seem to vary with change in orientation of the column (horizontal position, vertical position or inclined position). For a fixed probe length, the residence time is constant for the same packing material and flow rate. Similarly, the experimental residence times were unaffected by the type of packing material used (sand or angular rock fragments). However, for the same packing material the experimental residence times approximately halved when the flow rate increased from 25 ml/min to 50 ml/min, as expected. Table 4.4 summarizes collected data from the column in the horizontal position with sand packing at a flow rate of 25 ml/min. For probe 1, the experimental residence time was found to be 95.23 min. The calculated

4.3 Discussion

Fitting of the partial mixing model, described by Equation (2) and the axial dispersion model described by Equation (3), to the experimental data obtained from the column yielded the "experimental" values of the mixing efficiency, dispersion coefficient, and mean residence times. The residence time of groundwater flow can be calculated directly using Equation (1). This residence time will be called the "calculated" residence time in this study. The volumetric flow rate Q and the total volume of mobile water (V_T) available for the tracer in the system, are obtained from the experimental apparatus. The volumetric flow rates used in this study were 25 ml/min and 50 ml/min. The total volume of mobile water can be calculated by finding the product of the total volume of the column and the porosity of the packing material used. Comparing the experimental residence times obtained from both models with the calculated residence time values, showed slight variation. Table 4.37 lists the experimental and calculated values.

The experimental residence time values did not seem to vary with change in orientation of the column (horizontal position, vertical position or inclined position). For a fixed probe length, the residence time is constant for the same packing material and flow rate. Similarly, the experimental residence times were unaffected by the type of packing material used (sand or angular rock fragments). However, for the same packing material the experimental residence times approximately reduced by half when the flow rate increased from 25 ml/min to 50 ml/min, as expected. Table 4.1 shows data collected from the column in the horizontal position with sand packing at a flow rate of 25 ml/min. For probe 1, the experimental residence time was found to be 95.23 min. The calculated

residence time for this probe was found to be 98 min, using a porosity value of 0.4 for sand. Table 4.10 shows data collected from the column in a horizontal position with sand packing at a flow rate of 50 ml/min. The experimental residence time for probe 1 was found to be 55.82 min. The calculated residence time for the same probe was found to be 50 min using a porosity of 0.4 for sand. Comparing the value 55.82 min with the one found earlier for the same probe but with a flow rate of 25 ml/min, which is 95.23 min, it can be seen that the residence time for a flow rate of 50 ml/min is almost one half of that found with a flow rate of 25 ml/min for the same probe and same packing material. Table 4.37 compares the calculated residence times and the average experimental residence time values for three probes. The latter are the average values of the three positions (horizontal, vertical, inclined) for each probe. Figures 4.37 and 4.39 show that the experimental and calculated residence times compare very well.

Flow rate (ml/min)	Packing	Probe	Calculated residence time (min)	Experimental residence time (min)
25	Angular rock fragments	1 (35 cm)	123.63	124.18
		2 (60 cm)	211.25	214.24
		3 (85 cm)	300.26	296.18
50	Angular rock fragments	1 (35 cm)	61.81	55.82
		2 (60 cm)	105.97	95.23
		3 (85 cm)	150.13	136.04

Table 4.37: Comparison of the experimental residence times obtained from both models with the calculated residence times.

Flow rate (ml/min)	Packing	Probe	Calculated residence time, min	Average experimental residence time, min
25	Sand	1 (35 cm)	98.91	95.63
		2 (60 cm)	169.56	180.15
		3 (85 cm)	240.21	255.26
50	Sand	1 (35 cm)	49.45	55.19
		2 (60 cm)	84.78	91.90
		3 (85 cm)	120.10	144.76
25	Angular rock fragments	1 (35 cm)	123.63	108.08
		2 (60 cm)	211.95	192.71
		3 (85 cm)	300.26	284.54
50	Angular rock fragments	1 (35 cm)	61.81	61.33
		2 (60 cm)	105.97	99.54
		3 (85 cm)	150.13	154.69

Figure 4.38: Comparison between experimental and calculated residence times at flow rates of 25 ml/min and 50 ml/min using angular rock fragments as packing material.

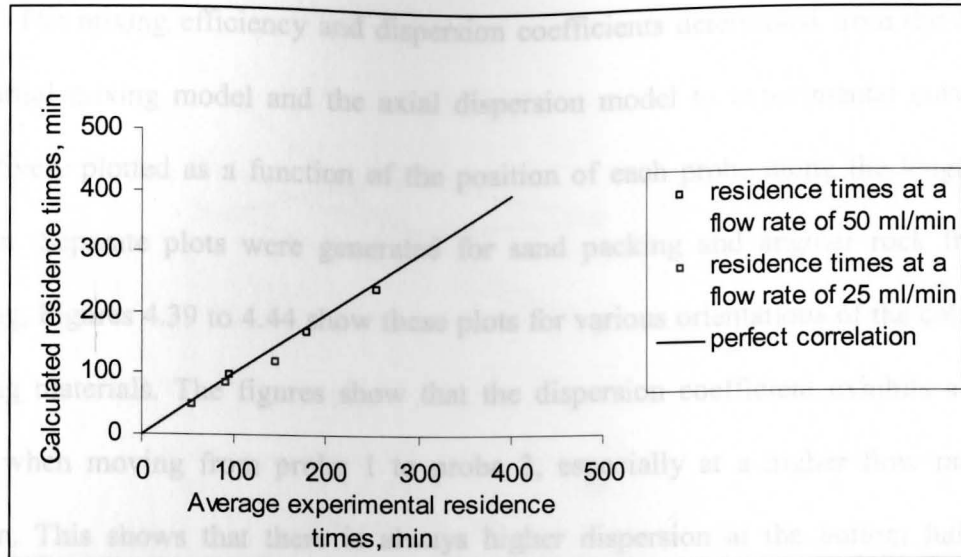


Figure 4.37: Comparison between experimental and calculated residence times at flow rates of 25 ml/min and 50 ml/min using sand as packing material.

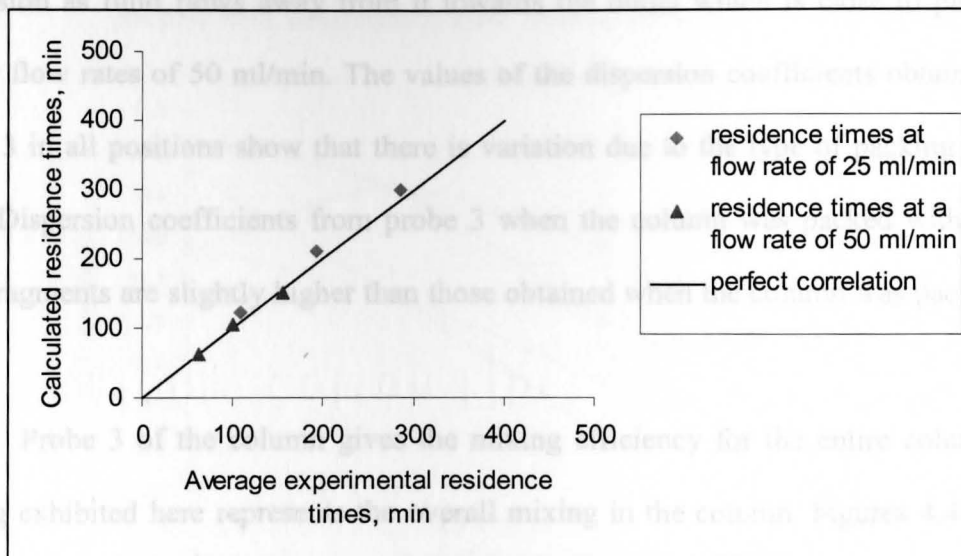


Figure 4.38: Comparison between experimental and calculated residence times at flow rates of 25 ml/min and 50 ml/min using angular rock fragments as packing material.

The mixing efficiency and dispersion coefficients determined from the fitting of the partial mixing model and the axial dispersion model to experimental curves were collectively plotted as a function of the position of each probe along the length of the column. Separate plots were generated for sand packing and angular rock fragments packing. Figures 4.39 to 4.44 show these plots for various orientations of the column and packing materials. The figures show that the dispersion coefficient exhibits a drop in value when moving from probe 1 to probe 3, especially at a higher flow rate of 50 ml/min. This shows that there is always higher dispersion at the bottom half of the column compared to its top half. In other words, since probe 1 was placed close to the inlet, it can be deduced that there is high dispersion near the inlet to the column and low dispersion as fluid flows away from it towards the outlet which is close to probe 3 at higher flow rates of 50 ml/min. The values of the dispersion coefficients obtained from probe 3 in all positions show that there is variation due to the type of packing material used. Dispersion coefficients from probe 3 when the column was packed with angular rock fragments are slightly higher than those obtained when the column was packed with sand.

Probe 3 of the column gives the mixing efficiency for the entire column. The mixing exhibited here represents the overall mixing in the column. Figures 4.44 – 4.49 show that the mixing efficiency values from probe 3 remain unaffected by the change in orientation, flow rates and packing material. This is to be expected since the mixing efficiency is by definition a constant that characterizes the average value of mixing in the system.

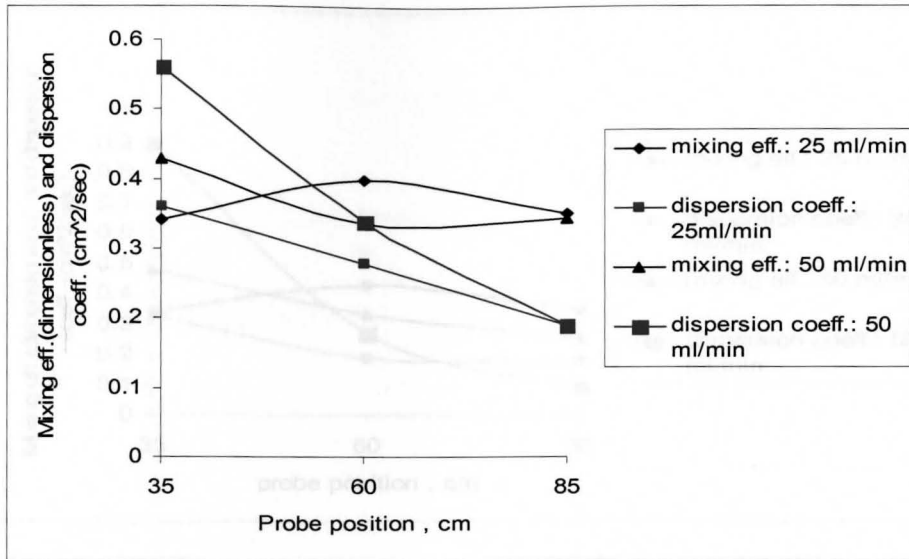


Figure 4.39: Variation of mixing efficiency and dispersion coefficient values as a function of probe position when column in horizontal position is packed with sand and at flow rates of 25 ml/min and 50 ml/min.

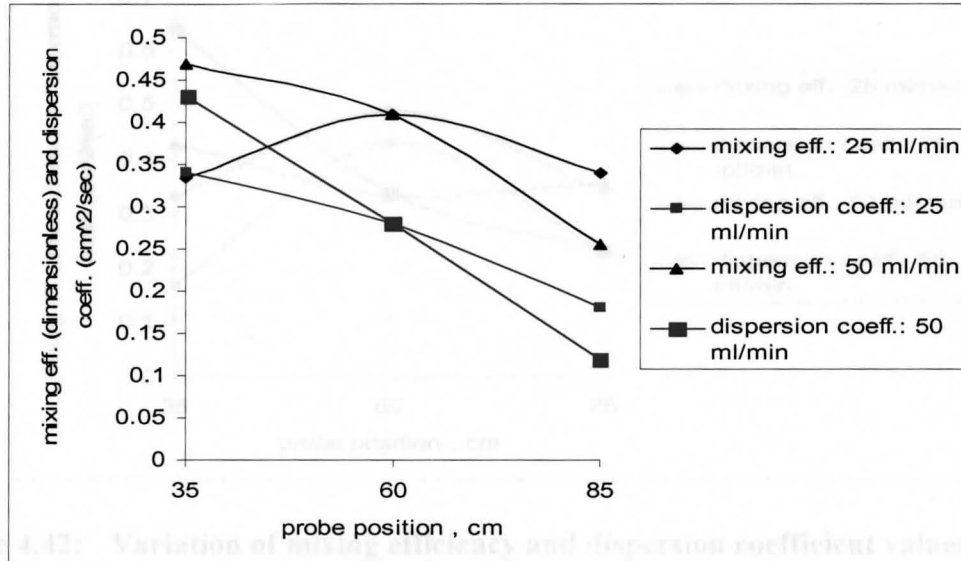


Figure 4.40: Variation of mixing efficiency and dispersion coefficient values as a function of probe position when column in vertical position is packed with sand and at flow rates of 25 ml/min and 50 ml/min.

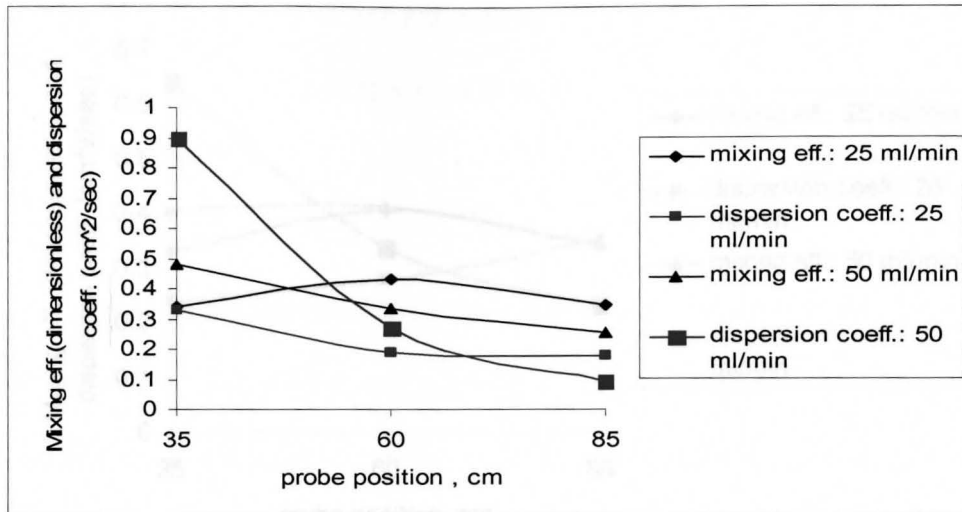


Figure 4.41: Variation of mixing efficiency and dispersion coefficient values as a function of probe position when column in inclined position is packed with sand and at flow rates of 25 ml/min and 50 ml/min.

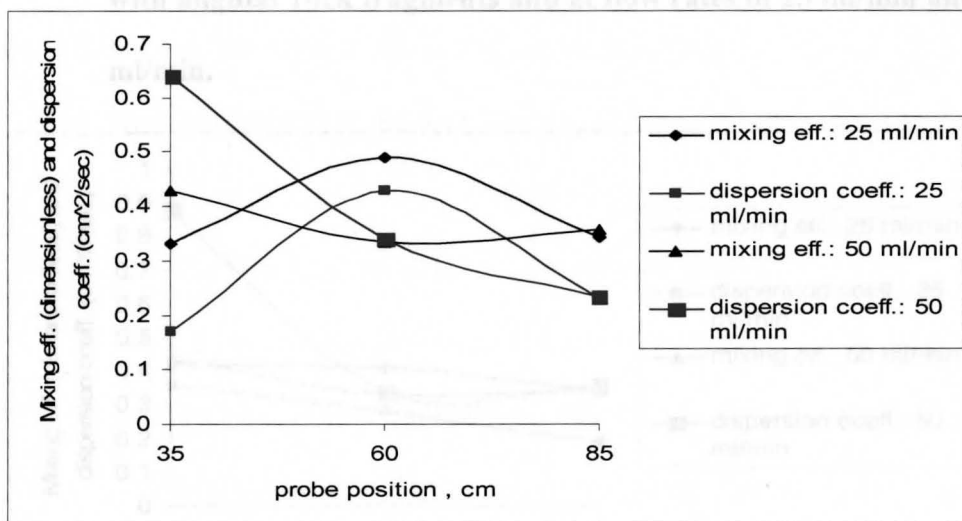


Figure 4.42: Variation of mixing efficiency and dispersion coefficient values as a function of probe position when column in horizontal position is packed with angular rock fragments and at flow rates of 25 ml/min and 50 ml/min.

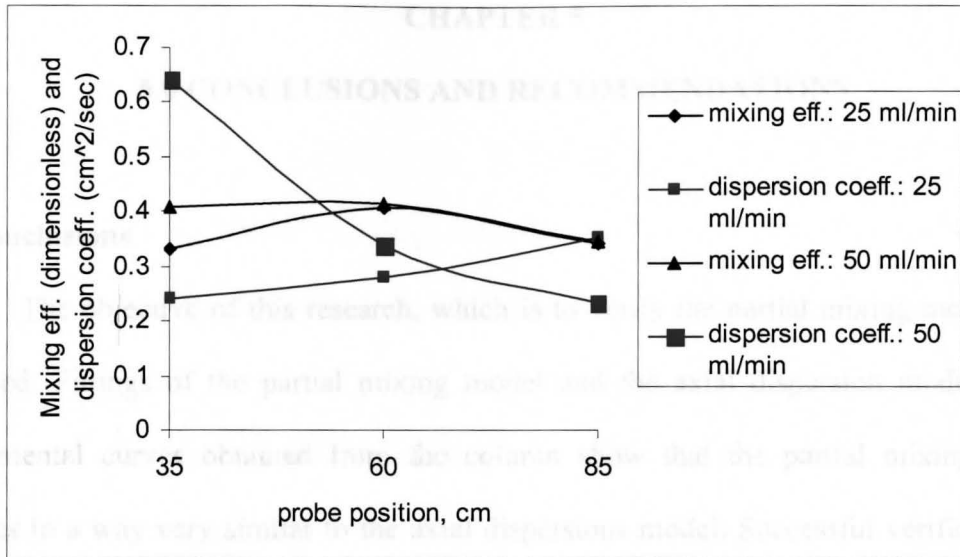


Figure 4.43: Variation of mixing efficiency and dispersion coefficient values as a function of probe position when column in vertical position is packed with angular rock fragments and at flow rates of 25 ml/min and 50 ml/min.

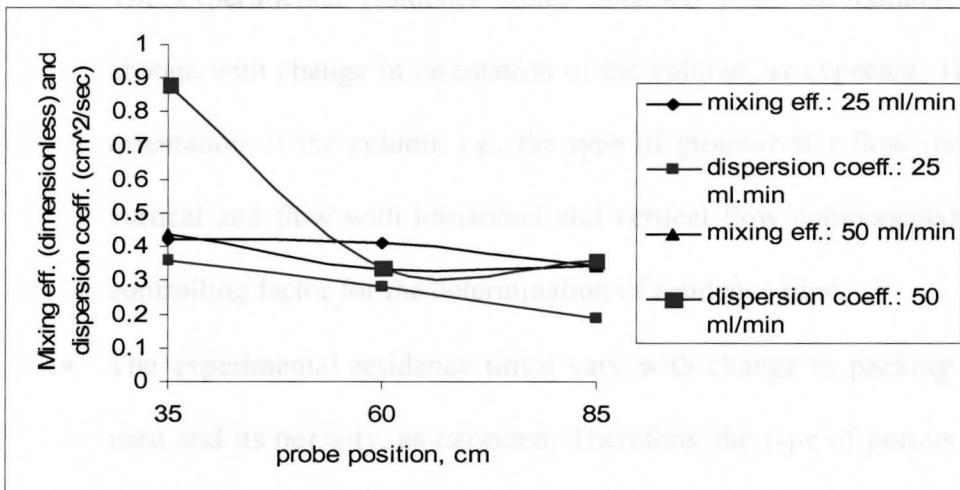


Figure 4.44: Variation of mixing efficiency and dispersion coefficient values as a function of probe position when column in inclined position is packed with angular rock fragments and at flow rates of 25 ml/min and 50 ml/min.

CHAPTER 5

5.0 CONCLUSIONS AND RECOMMENDATIONS

5.1 Conclusions

The objective of this research, which is to verify the partial mixing model, was achieved. Fittings of the partial mixing model and the axial dispersion model to the experimental curves obtained from the column show that the partial mixing model behaves in a way very similar to the axial dispersions model. Successful verification of the partial mixing model using simple laboratory-controlled experiments in this study confirm the fact that the partial mixing model will produce accurate and reliable data when applied to the natural more complex systems of groundwater.

The following conclusions can be made from this study:

- The experimental residence times obtained from the column did not change with change in orientation of the column, as expected. Therefore, orientation of the column i.e., the type of groundwater flow (horizontal, vertical and flow with horizontal and vertical flow components) is not a controlling factor for the determination of residence time.
- The experimental residence times vary with change in packing material used and its porosity, as expected. Therefore, the type of porous medium and its porosity are controlling factors for determination of the residence time.
- As expected, experimental residence times obtained at a flow rate of 25 ml/min are almost twice those obtained at a flow rate of 50 ml/min.

- Comparison of the experimental and calculated values of residence times shows little variation, thus indicating accurate experimental simulation of mixing in the column.
- Mixing efficiency values did not change with change in orientation of the column, change in flow rates, and change in the type of packing material used.
- Dispersion coefficient values varied with change in packing material used in the column.
- Dispersion coefficient values showed a drop when moving from probe 1 to probe 3 in the column, and are more pronounced at higher flow rates (50 ml/min).

5.2 Future recommendations

This study was conducted using a one meter long poly-carbonate column with sand packing and then later with angular rock fragments packing. To increase the scope of this study, a column longer than one meter can be used. Future studies can incorporate other types of packing material. This study involved using two flow rates of 25 ml/min and 50 ml/min. Studies with lower flow rates, e.g., 5 ml/min and/or 10 ml/min, can be used to achieve higher mixing efficiency values. Variations in values of mixing efficiency can be achieved by varying flow rates, e.g., starting from a flow rate of 5 ml/min to 50 ml/min in increments of 5 ml/min.

In this study, the first set of experiments was conducted with sand packing alone, and the second set with angular rock fragments alone. In the future, studies can include a

mixture of sand and angular rock fragments or sand and gravel to observe different mixing patterns. When packing the column with two different materials at the same time, one of two methods can be adopted or both. Sand and angular rock fragments can be mixed uniformly before filling the column or the column can be divided into two halves where one half can be occupied with sand and the other with angular rock fragments. This will allow simulation of mixing in porous media with more complicated heterogeneities.

The suitability of the partial mixing model in laboratory controlled experiments using a packed column with a step input can be analyzed. A step input of the tracer can be achieved by allowing fresh water to pass through the column till a steady state is observed through conductivity readings, and then allowing the tracer to pass through the column continuously till a new steady state much higher than the earlier one is observed through conductivity readings. The partial mixing model can be made to fit these experimental curves with a step input of the tracer with slight modifications.

Future research can involve analyzing the suitability of the partial mixing model in natural systems where the aquifer is already contaminated and the nature of input is unknown. The partial mixing model in the current study is applied only to an impulse injection of tracer. The applicability of the partial mixing model to other types of inputs will give a better understanding of the model and mixing patterns.

Future studies can involve reproducing this laboratory experiment in a field setting. The research would apply the partial mixing model to a natural aquifer that is already contaminated. The research would install four wells along a specific length and at a specified separation. This section of the aquifer would be tested in a way similar to the

column used in the laboratory experiments. Drilling and sampling would determine the extent of the aquifer. The wells would fully penetrate the depth of the aquifer. Horizontal, inclined or vertical flow represents would establish a three dimensional flow regime. The partial mixing model can then be applied to this setting to determine the mean residence times and mixing efficiency values for the natural system.

Carroll, M. J., 1977. A study of the effects of transport phenomena in natural systems. Ph.D. dissertation, University of Arizona, Tucson, Arizona, 217 pp.

Carroll, M. J., 1978. The use of tritium for estimating groundwater storage. *Water Resour. Res.*, 14(4), pp. 151-176.

Himmelblau, D.M., and K. B. Redden, 1963. Process analysis and simulation. *Journal of Applied Chemistry*, John Wiley and Sons, New York, 342 pp.

Hill, C. G., 1977. A reconsideration to chemical engineering kinetics and reactor design. John Wiley and Sons, New York.

Michalewski, P., and A. Zuber, 1982. Determining the number of cells of ground water systems with the aid of environmental tracers. I. Methods and their applicability. *Journal of Hydrology*, 59(1-4), pp.207-231.

Wat, A., 1964. On the interpretation of tritium "age" measurements in ground water. *Journal of Geophysical Research*, 69(12), pp. 2194-2195.

REFERENCES

- Amin, I.E., 1987. A general mathematical model for the interpretation of tracer data and calculation of transit times in hydrologic systems. Ph.D. dissertation, University of Nevada – Reno.
- Amin, I.E. and M.E. Campana, 1996. A general lumped parameter model for the interpretation of tracer data and transit time calculation in hydrologic systems. *Journal of Hydrology*, Vol. 179, pp. 1-21.
- Campana, M.E., 1975. Finite-state models of transport phenomena in hydrologic systems. Ph.D. dissertation, University of Arizona, Tucson, Arizona, 252 pp.
- Eriksson, E., 1958. The possible use of tritium for estimating groundwater storage. *Tellus*, 10(4), pp. 472-478.
- Himmelblau, D.M. and K.B. Bischoff, 1968. *Process analysis and simulation: deterministic systems*. John Wiley and Sons, New York, 348 pp.
- Hill, C.G., 1977. *An introduction to chemical engineering kinetics and reactor design*. John Wiley and Sons, New York.
- Maloszewski, P., and A. Zuber, 1982. Determining the turnover time of groundwater systems with the aid of environmental tracers, 1. Models and their applicability. *Journal of Hydrology*, 57(3/4), pp.207-231.
- Nir, A., 1964. On the interpretation of tritium “age” measurements of groundwater. *Journal of Geophysical Research*, 69(12), pp. 2589-2595.

- Przewski, K. and Y. Yurtsever, 1974. Some conceptual mathematical models and digital simulation approach in the use of tracers in hydrologic systems. In: Isotope Techniques in Groundwater, Vol. II, International Atomic Energy Agency, Vienna, pp. 425-450.
- Simpson, E.S. and L. Duckstein, 1976. Finite-state mixing cell models. In: Yevjevich, V., editor, Karst Hydrology and Water Resources. Water Resources Publications, Fort Collins, Colorado, pp. 489-512.
- Zuber, A., 1985. Review of existing mathematical models for interpretation of tracer data in hydrology. Institute of Nuclear Physics Report No. 1270/AP, Cracow, Poland, 59 pp.
- Zuber, A., 1986. Mathematical models for the interpretation of environmental radioisotopes in groundwater systems. In: Fritz, P. and J.Ch. Fontes, editors, Handbook of Environmental Isotope Geochemistry, Vol 2. Elsevier, Amsterdam, pp. 1-60